FACULTY
OF MATHEMATICS
AND PHYSICS
Charles University

DOCTORAL THESIS

Josef Melcr

Simulation of processes in cellular membranes

Institute of Organic Chemistry and Biochemistry v.v.i., AS CR

Advisor of the thesis:	prof. Pavel Jungwirth
Study programme:	Physics
Study branch:	Biophysics, chemical and macromolecular physics

Prague 2018

I declare that I carried out this doctoral thesis independently, and only with the cited sources, literature and other professional sources.

I understand that my work relates to the rights and obligations under the Act No. 121/2000 Sb., the Copyright Act, as amended, in particular the fact that the Charles University has the right to conclude a license agreement on the use of this work as a school work pursuant to Section 60 subsection 1 of the Copyright Act.

In .... date .... signature of the author

“It’s a dangerous business, Frodo, going out of your door,” he used to say. “You step into the Road, and if you don’t keep your feet, there is no telling where you might be swept off to.” (J. R. R. Tolkien)

To all people, who helped us on this adventurous journey.

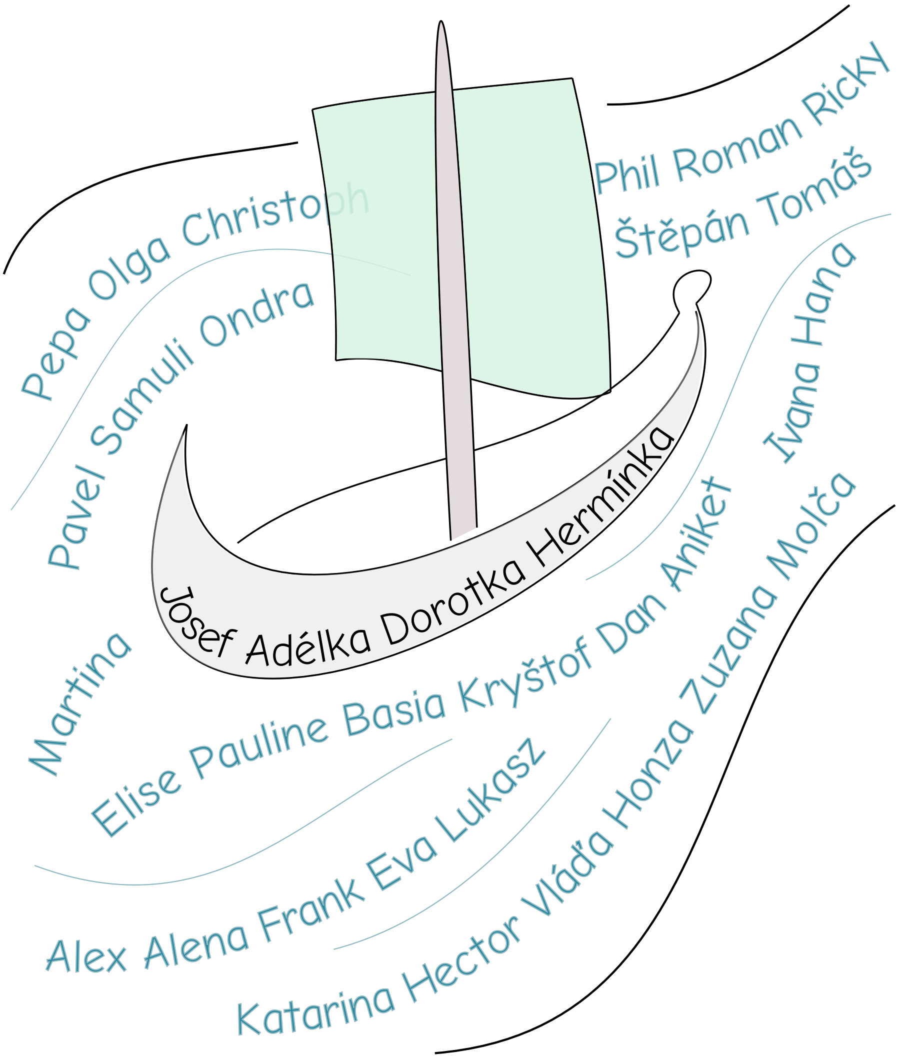
Pepa Olga Christoph
Pavel Samuli Ondra
Phil Roman Ricky
Štěpán Tomáš
Ivana Hana
Josef Adélka Dorotka Hermínka
Martina
Elise Pauline Basia Kryštof Dan Aniket
Alex Alena Frank Eva Lukasz
Katarina Hector Vláďa Honza Zuzana Molča

I am grateful to you for all you have done for me. I especially thank to my PhD advisor Pavel Jungwirth for the amazing period of my life full of exciting science, and for the great support to my scientific carrier as well as our family life. I thank Samuli Ollila for the stimulating scientific discussions. I cannot express enough gratitude to my wife Adéla and to our two daughters Dorotka a Hermínka, who fuelled me with love, vigour and happiness. My special thanks belong to our families for their immense support and encouragement.

Title: Simulation of processes in cellular membranes

Author: Josef Melcr

Institute: Institute of Organic Chemistry and Biochemistry v.v.i., AS CR

Advisor: prof. Pavel Jungwirth, Department of physical and macromolecular chemistry

Abstract: Many important processes in cells involve ions, e.g., fusion of synaptic vesicles with neuronal cell membranes is controlled by a divalent cation Ca^{2+}; and the exchange of Na^+ and K^+ drives the the fast electrical signal transmission in neurons. We have investigated model phospholipid membranes and their interactions with these biologically relevant ions. Using state-of-the-art molecular dynamics simulations, we accurately quantified their respective affinites towards neutral and negatively charged phospholipid bilayers. In order to achieve that, we developed a new model of phospholipids termed ECC-lipids, which accounts for the electronic polarization via the electronic continuum correction implemented as charge rescaling. Our simulations with this new force field reach for the first time a quantitative agreement with the experimental lipid electrometer concept for POPC as well as for POPS with all the studied cations. We have also examined the effects of transmembrane voltage on phospholipid bilayers. The electric field induced by the voltage exists exclusively in the hydrophobic region of the membrane, where it has an almost constant strength. This field affects the structure of nearby water molecules highlighting its importance in electroporation.

Keywords: molecular dynamics simulations, molecular modeling, polarizability, biological membranes, phospholipid bilayers, phosphatidylcholine transmembrane potential, sodium, potassium, calcium

Contents

Preface **3**

1 Biological membranes **5**
1.1 Interactions of cations with phospholipid bilayers 5
1.2 NMR molecular electrometer concept 6

2 Molecular modeling of biological membranes **9**
2.1 Classical molecular dynamics simulations 9
2.2 Electronic continuum correction as implicit treatment of electronic polarizability 11
2.3 Implicitly polarizable classical MD models of lipids using ECC . . 12
2.3.1 Structural parameters of model membranes with ECC-lipids: Agreement with experiments 14
2.4 Modeling of transmembrane potential 17

3 Interactions of ions with phospholipid bilayers **21**
3.1 Binding of cations to phospholipid bilayers and lipid electrometer concept from experiments and simulations 21
3.2 Interactions of neutral and negatively charged phospholipid membranes with Na^+ and K^+ cations 25
3.3 Interactions of neutral and negatively charged phospholipid membranes with Ca^{2+} cations 31

Conclusion **41**

Bibliography **43**

List of Figures **58**

List of Tables **62**

List of Abbreviations **63**

List of publications and attachments **65**

Preface

Cellular membranes are important and evolutionarily very old biological structures. [Alberts et al., 2008] The first primitive predecessors of cells already bear hints of membranes separating their inner environment from the outer world. Current organisms often contain a multitude of immensely complex membranes, each serving many functions. Processes in cellular membranes are thus crucial for life.

My work is motivated by processes, which involve interactions of biologically relevant ions with cellular membranes. For instance in neurons, the fusion of synaptic vesicles containing neurotransmitter with neuronal cell membranes is controlled by a divalent cation Ca^{2+}. [Berridge et al., 2003, Clapham, 2007] This process is triggered by a change in the transmembrane potential across the neuronal plasma membrane, which is modulated by the exchange of the monovalent cations Na^{+} and K^{+}. [Sten-Knudsen, 2002] The transmembrane potential in atomistic simulations can be modeled by two approaches, the constant electric field method, and the ion-imbalance method. The methodological differences between them raise the following questions: Do they provide the same results? Can they be used interchangeably? What happens to the membrane under voltage?

Until recently, there was no consensus on the binding of Na^{+}, K^{+}, and Ca^{2+} cations to biological membranes – simulations and some experiments [Berkowitz and Vacha, 2012, Vacha et al., 2009, Harb and Tinland, 2013] do not reproduce other experiments [Roux and Bloom, 1990, Pabst et al., 2007, Akutsu and Seelig, 1981]. From the point of simulations, all currently available models require improvements to reproduce quantitatively structures and interactions with cations. Here, the following questions arise: Is the missing electronic polarization in standard non-polarizable simulations responsible for the discrepancy? If yes, how crucial is it for the interactions of phospholipid bilayers with biologically relevant cations, and can it be effectively accounted for by rescaling charges? Can we obtain in this way realistic structures of phospholipid bilayers with interacting cations at atomistic resolution?

1. Biological membranes

All living cells separate their inner environment from the exterior by a membrane preventing molecules from a free diffusion in or out. This allows the cells to maintain specific conditions required for their functioning. Cellular membranes are mainly composed of lipids and proteins, while enrichment with other molecules, e.g., sugars and saccharides forming glycocalyx, is often required for their specific function. [Reitsma et al., 2007] In such a dynamically structured fluid mosaic, lipids self-assemble into a lipid bilayer [Vereb et al., 2003, Mouritsen, 2011, Vattulainen and Rog, 2011].

Biological membranes are systems with a very complex structure. It is, hence, convenient to use simplified models of such membranes, which allow us to focus on the basic principles and properties. Lipid bilayers are often used as such model membranes being accessible for both experimental and simulation studies. In particular, the zwitterionic phosphatidylcholine (PC) bilayers are used to study the role of ions in complex biological systems [Scherer and Seelig, 1987, Seelig, 1990, Cevc, 1990, Vacha et al., 2009, Javanainen et al., 2017]. In experiments, there are several commonly used model membrane systems – liposomes, micelles, unilamellar vesicles of varying sizes from giant to small, supported bilayers, bicelles, and nanodiscs. [Oluwole et al., 2017, Alberts et al., 2008, Marsh, 2013] Despite their simplicity compared to cellular membranes, even such model membranes pose significant challenge for science today. [Tarun et al., 2018, Melcrová et al., 2016, Javanainen et al., 2017, Magarkar et al., 2017, Botan et al., 2015, Catte et al., 2016, Kulig et al., 2015, 2014, Pluháčková et al., 2016, Vacha et al., 2009]

1.1 Interactions of cations with phospholipid bilayers

Interactions of cations with cellular membranes play a key role in many biological processes. The binding of Na^+ and Ca^{2+} to PC bilayers has been widely studied both in experiments [Akutsu and Seelig, 1981, Altenbach and Seelig, 1984, Seelig, 1990, Cevc, 1990, Tocanne and Teissié, 1990, Binder and Zschörnig, 2002, Pabst et al., 2007, Uhríková et al., 2008] and simulations [Magarkar et al., 2017, Böckmann et al., 2003, Böckmann and Grubmüller, 2004, Berkowitz and Vacha, 2012, Melcrová et al., 2016, Javanainen et al., 2017, Catte et al., 2016, Bacle et al., 2018]. The details of ion binding are, however, not fully consistent in the literature. The relative binding affinities of ions are generally agreed to follow the Hofmeister series [Eisenberg et al., 1979, Cevc, 1990, Tocanne and Teissié, 1990, Binder and Zschörnig, 2002, Garcia-Celma et al., 2007, Leontidis and Aroti, 2009, Vacha et al., 2009, Klasczyk et al., 2010, Harb and Tinland, 2013], however, there is no consensus on the quantitative aspects of the ion affinities.

Interpretations of spectroscopic methods, like nuclear magnetic resonance (NMR), x-ray scattering, and infrared spectroscopy suggest that monovalent alkali cations (with the exception of Li^+) exhibit negligible binding to PC lipid bilayers, while multivalent cations interact more strongly [Cevc, 1990, Tocanne and Teissié, 1990, Hauser et al., 1976, 1978, Herbette et al., 1984, Altenbach and Seelig, 1984, Uhríková et al., 2008]. In particular, submolar concentrations of NaCl have a negligible effect on phospholipid infrared spectra [Binder and Zschörnig, 2002], area per molecule [Pabst et al., 2007], dipole potential [Clarke and Lüpfert, 1999], lateral diffusion [Filippov et al., 2009], and choline head group order parameters [Akutsu and Seelig, 1981];

Another view, emerging more recently, suggests much stronger interactions between phospholipids and monovalent cations. For instance, submolar concentrations of NaCl reduce rotational and translational dynamics of membrane-embedded fluorescent probes [Böckmann et al., 2003, Vacha et al., 2009, Harb and Tinland, 2013], and changes in the hardness of bilayers are also reported from atomic force microscopy experiments [Garcia-Manyes et al., 2005, 2006, Fukuma et al., 2007, Ferber et al., 2011, Redondo-Morata et al., 2012]. In addition, atomistic molecular dynamics simulations consistently predict strong interactions of Na^+ with phospholipids bilayers, which, however, depend on the employed model [Böckmann et al., 2003, Böckmann and Grubmüller, 2004, Sachs et al., 2004b, Berkowitz et al., 2006, Cordomí et al., 2008, 2009, Valley et al., 2011, Berkowitz and Vacha, 2012, Catte et al., 2016, Bacle et al., 2018, Melcr et al., 2018].

In our recent work [Catte et al., 2016], we addressed the apparent controversies using the molecular electrometer concept, where the experimentally (by NMR) measured changes of certain head group order parameters are related to the amount of charge bound to a bilayer. [Brown and Seelig, 1977, Akutsu and Seelig, 1981, Altenbach and Seelig, 1984, Seelig et al., 1987, Scherer and Seelig, 1989]. This concept is introduced and further discussed in the following section 1.2. We have shown that the response of the PC head group order parameters α and β to cations bound to the bilayer is qualitatively correct in MD simulations, but several models grossly overestimate the affinity of Na^+ to such bilayers. Moreover, we find that the interactions of Ca^{2+} cations with PC bilayers in current simulation models are not accurate enough for interpreting NMR experiments. We argued that the lack of electronic polarizability in the simulations can be responsible for the disagreement. Consequently, we developed a model of POPC, which accounts for electronic polarization through electronic continuum correction (see section 2.2), and which yields accurate response of the head group order parameters to various monovalent and divalent cations. [Melcr et al., 2018] This model was also extended to other lipids, which are introduced in the section 2.3, and it was employed in Chapter 3 providing a simulation-based supporting evidence to the older view, which suggests that Na^+ and K^+ interact weakly, while Ca^{2+} specifically binds to phospholipid bilayers.

1.2 NMR molecular electrometer concept

Ion binding in lipid bilayers can be experimentally quantified by measuring the changes of the head group order parameters in lipids. In the case of the head group order parameters α and β in phosphatidylcholine (see Fig. 2.1 for the definition of the order parameters) such changes are known under the term "electrometer concept" [Seelig et al., 1987, Catte et al., 2016, Ollila and Pabst, 2016]. It is experimentally observed that the C-H bond order parameters of α and β carbons in a PC lipid head group are proportional to the amount of charge, positive or negative, bound per lipid [Seelig et al., 1987]. The change of the order parameters measured with varying concentrations of aqueous ions can be then related to the amount of bound ions.

The order parameters can be robustly and accurately determined from both MD simulations and NMR experiments. Hence, the electrometer concept can be used to compare the two techniques in terms of the ion binding affinities to lipid bilayers containing PC phospholipids. [Catte et al., 2016, Ollila and Pabst, 2016]

From MD simulations the order parameters can be calculated using the definition

$$S_{\mathrm{CH}} = \frac{1}{2}\langle 3\cos^2\theta - 1\rangle, \tag{1.1}$$

where θ is the angle between the C−H bond and membrane normal and the average, denoted with pointed brackets, is taken over all sampled configurations [Ollila and Pabst, 2016].

The order parameters for all C-H bonds in lipid molecules, including α and β segments in head group, can be accurately measured using ^{2}H or ^{13}C NMR techniques [Ollila and Pabst, 2016]. The relation between the amount of the bound charge per lipid, $X^{\pm}$, and the head group order parameter change, ΔS^i_{CH}, is empirically quantified as [Seelig et al., 1987, Ferreira et al., 2016]

$$\Delta S^i_{\mathrm{CH}} = S^i_{\mathrm{CH}}(X^{\pm}) - S^i_{\mathrm{CH}}(0) \approx m_i \frac{4}{3\chi} X^{\pm}, \tag{1.2}$$

where $S^i_{\mathrm{CH}}(0)$ denotes the order parameter in the absence of any bound charge, i refers to either α or β carbon, m_i is an empirical constant depending on the valency and the position of the bound charge, and $\chi \approx 167\,\mathrm{kHz}$ is the quadrupole coupling constant, with the experimental value for POPC from the works by Seelig and Seelig [1977], Davis [1983].

The measured change of the order parameter depends on the head group response to the bound charge and on the amount of the bound charge (*i.e.,* m_i and $X^{\pm}$ in Eq. 1.2, respectively). The quantification of the empirical factor m_i has been done experimentally for a wide range of systems to demonstrate the robustness of the electrometer concept and its negligible chemical specificity [Seelig et al., 1987, Beschiaschvili and Seelig, 1991]. The measurements of the electrometer response to cationic surfactants can be exploited in simulations to compare the response of the head group order parameters with a known amount of bound surface charge per lipid, i.e., $X^{\pm}$ in Eq. 1.2, as all molecules of the surfactant partition into the bilayer.

2. Molecular modeling of biological membranes

Biological membranes are difficult to study experimentally due to their complex character. Among the well established methods for the studies of membranes belong NMR [Catte et al., 2016, Botan et al., 2015, Wohlgemuth et al., 1980, Seelig, 1990, Seelig et al., 1987], small angle x-ray diffraction (SAXD) [Ollila and Pabst, 2016, Pabst et al., 2007], and fluorescence spectroscopy [Javanainen et al., 2017, Melcrová et al., 2016, Vacha et al., 2009]. Recent advances in cryo-EM [Chiu and Downing, 2017, Nogales, 2015] and single-molecule microscopy imaging [Ritchie et al., 2013] reveal another promising tools. The resolution of such experimental methods is, however, often insufficient for the characterization of the structure in atomistic detail. In contrast, molecular dynamics simulations provide atomistic resolution of biomolecules. This makes simulations well suited to be used in conjunction with the experimental methods bringing deeper insight to the experimentally determined properties. In addition, the properties from experiments can be extracted from the simulations and compared together, thus cross-validating the two independent approaches.

Starting with simple membrane models [Berger et al., 1997, Böckmann and Grubmüller, 2004, Böckmann et al., 2003, Sachs et al., 2004b,a] simulations of membranes have evolved into a field of computational biophysics that is capable of answering fundamental questions like how divalent cations modulate the signalling function of PI(4,5) P_2 [Bilkova et al., 2017]; whether there is any preference of calcium cations towards flat plasma membrane or curved synaptic vesicles [Magarkar et al., 2017]; or what are the exchange pathways of plastoquinone and plastoquinol in the photosystem II complex in Thylakoid membranes [Van Eerden et al., 2017]. Recent progress in computational resources and algorithms has allowed the simulations to grow in spatial scales and composition complexity enabling relevant applications in biology. [Friedman et al., 2018]

2.1 Classical molecular dynamics simulations

In a MD simulation, the system of interest is propagated numerically in discrete time steps using the Newton equations of motion. Interactions between particles, which often represent individual atoms, are described by an approximate interaction potential, U, also called a *force field*. Such a potential can be formally written as a sum of individual terms representing different model interactions. The symbols K are the force constants describing the strengths of the bonded interactions, which are formally written as

$$\begin{aligned} U = \quad & \sum_{bonds} K_b(r-r_0)^2 + \sum_{angles} K_\Theta(\Theta-\Theta_0)^2 + \\ & \sum_{dihedrals} K_n(1+\cos(n\phi-\phi_0)) + \\ & \sum_{i<j}\left(s_{ij}^{VdW} 4\epsilon_{ij}\left[\left(\frac{\sigma_{ij}}{r_{ij}}\right)^{12} - \left(\frac{\sigma_{ij}}{r_{ij}}\right)^{6}\right] + s_{ij}^{q}\frac{q_i q_j}{\epsilon\, r_{ij}}\right) \end{aligned} \tag{2.1}$$

The first three terms represent the intra-molecular forces arising from bond stretching, angle bending, and dihedral angle torsion. r, Θ and ϕ are their respective dimensions, and n is the multiplicity of the torsion potential.

The last terms in the large brackets represent the inter-molecular interactions; Van der Waals and electrostatic forces. Depending on the model force field, the non-bonded interactions are not evaluated between atoms that are connected by less than three or four bonds, which is here formally introduced through the matrix s_{ij} that modifies the interactions accordingly.

The interactions representing the attractive dispersion and the repulsive excluded volume in the empirical interaction potential in Equation 2.1 adopt typically the form of Lennard-Jones potential. It is expressed in terms of the interaction energy ϵ_{ij}, and σ_{ij}, which is the distance, where the potential crosses zero. As the forces at the distances smaller than σ_{ij} are strongly repulsive, these parameters thus also report on the size of the spherical particles having an impact on the balance of Van der Waals forces with electrostatic forces.

The electrostatic interaction creates strong attractive and repulsive forces. In classical MD simulation, it is approximated using point partial charges, q_i, in the centres of the particles (most often atoms). Forces from long distances yield non-negligible contributions, which must to be accounted for especially in the commonly used periodic systems, i.e., in simulations with periodic boundary conditions. In neutral systems, this is efficiently done by using the Ewald summation, in which the long range contributions are calculated in Fourier space rather than in real space using fast algorithms developed for this purpose. [Darden et al., 1993, Essman et al., 1995] The formally applied dielectric constant of the medium, ϵ, is assumed to be 1 in most force fields for biomolecules. In a later section 2.2, we will show how to modify this interaction by changing the dielectric constant ϵ to include the effects of electronic polarization.

Molecular dynamics simulations of biological membranes employ empirical particle-based models of molecules using the interaction potential, often termed force field, from Eq. 2.1. The models are built using classical non-polarizable particles, each representing an individual atom (atomistic models), or a group of atoms (united-atom or coarse-grained models). The following classical models are among the most popular in membrane modeling:

- Atomistic
  - CHARMM [Klauda et al., 2010]
  - Slipids [Jämbeck and Lyubartsev, 2012a,b]
  - OPLS lipids by Maciejewski et al. [2014]
  - Lipid14 [Dickson et al., 2014]
- United-atom models
  - Berger [Berger et al., 1997]
  - CHARMM-UA [Lee et al., 2014]
- Coarse-grained
  - MARTINI [Marrink et al., 2007]

Despite all successes and valuable insights that simulations have provided, there is still a large room for possible improvements of the current simulation models. For example, recent studies by Botan et al. [2015], Catte et al. [2016] have shown that both structures and interactions of phospholipid models require further optimization in order to become capable of interpreting solid state NMR experiments. In particular, we have discovered that the lack of electronic polarizability is a major issue in any of the models from the above mentioned studies when interactions with charged moieties become important. [Melcr et al., 2018] Several possible ways for including polarizability into simulations, both explicit and implicit, will be introduced in the following sections.

2.2 Electronic continuum correction as implicit treatment of electronic polarizability

The lack of electronic polarizability in classical MD simulations has been considered a serious issue since the early days of the modeling of lipid bilayers. There exist two main approaches for the explicit representation of electronic polarizability – atomic induced dipoles and Drude oscillators. The induced dipole approach models the polarizability through a point dipole moment on each atom. Such an electric dipole is induced by the acting electric field proportionally to its polarizability. This model is implemented in the widely adopted force field AMOEBA [Piquemal et al., 2006, Ponder et al., 2010, Shi et al., 2013].

The classical Drude oscillator model is inspired by a classical representation of a lone pair of electrons. It uses an auxiliary charge, also termed Drude oscillator or Drude particle, which is attached to each atom through a harmonic spring. The displacement of the Drude particle represents the induced polarization proportionally to the acting electric field, as implemented for example in the Drude force field [Lemkul et al., 2016].

Although the two approaches, the induced dipole model and the classical Drude oscillator model, are very different in how they represent polarizability in simulations, it was shown that the classical Drude oscillator formalism can be converted to the induced dipole formalism proving the two methods to be equivalent. [Huang et al., 2017] From the point of view of lipids, however, the classical models with fixed charges and no explicit polarizability that are currently available provide comparable accuracy at a fraction of the computational cost of the models with explicit polarization. [Lucas et al., 2012, Chowdhary et al., 2013]

Instead of the computationally demanding explicit polarization approach, electronic polarization can also be accounted for implicitly. Such an implicit mean field model of electronic polarizability termed Electronic continuum correction (ECC) was first suggested by Leontyev and Stuchebrukhov [2009], and was then systematically applied to solutions of ions by Pluhařová et al. [2014], Kohagen et al. [2014, 2016], Martínek et al. [2018]. Through a comparison of neutron scattering and/or *ab-initio* molecular dynamics data with classical MD simulations, the authors developed an array of models for cations and anions, termed here as ECC-ions, which provide realistic structures even for concentrated solutions of both monovalent and divalent cations.

In ECC, a system of polarizable particles is represented with an equivalent system of particles with fixed charges. This can be done by a simple transform of the partial charges, which does not change the form of the empirical force field in Equation 2.1, providing the effects of the electronic polarization in a mean field way at no additional computational cost. Although this is technically similar to the phenomenological scaling of partial charges applied in earlier studies of aqueous solutions or ionic liquids [Jönsson et al., 1986, Egberts et al., 1994, Beichel et al., 2014], ECC is a physically well justified and rigorously derived model [Leontyev and Stuchebrukhov, 2009, 2010, 2011, 2014]. Assuming that the electronic polarizability of electrons is approximately constant in biological solutions, it was shown by Leontyev and Stuchebrukhov [2011] that the electrostatic interactions between atoms are screened like in a dielectric continuum with an electronic dielectric constant, ϵ_{el}, also known as the high frequency dielectric constant. This can be formally written as

$$U = \frac{1}{2}\sum_{j\neq i}^{N} \frac{q_i q_j}{\epsilon_{el}\, r_{ij}} = \frac{1}{2}\sum_{j\neq i}^{N} \frac{\frac{q_i}{\sqrt{\epsilon_{el}}}\frac{q_j}{\sqrt{\epsilon_{el}}}}{r_{ij}}, \tag{2.2}$$

where q_i is the point charge of the particle i, and r_{ij} are the distances between particles i and j. It naturally follows from the above equation that embedding all atoms into a dielectric continuum is equivalent to a formal scaling of the atomic point charges

$$q_i^{ECC} = \frac{q_i}{\sqrt{\epsilon_{el}}}, \tag{2.3}$$

where q_i and q_i^{ECC} are respectively the original partial charges and the scaled charges, which represent the effects of the electronic polarization. Given that the high frequency dielectric constant of water is 1.78 (i.e., the square of the refraction index of 1.33), the scaling factor for ions in water is ≈ 0.75.

It is important to note that the value of the high frequency dielectric constant is around 2 for almost any biologically relevant environment [Leontyev and Stuchebrukhov, 2011]. This means that even interfaces like biological membranes do not contain discontinuities of the electronic continuum. The dielectric discontinuity in a lipid bilayer thus arises only from the orientational polarization of the molecules, which is accounted for explicitly in standard MD simulations. Therefore, the same correction for the electronic polarizability can be applied throughout the lipid bilayer/aqueous solution interface.

2.3 Implicitly polarizable classical MD models of lipids using ECC

Simulation studies have revealed that the interactions of phospholipids with cations, especially with divalent cations, are overestimated in all classical MD models. [Catte et al., 2016, Bacle et al., 2018] The neglect of polarizability in the simulations was one of the possible explanations for the observed discrepancy between simulations and experiments. Motivated by the accuracy and simplicity of the electronic continuum correction (ECC) applied on ions by [Martínek et al., 2018], we developed implicitly polarizable models of phospholipids using a similar strategy. The newly developed model provides accurate interactions between phospholipid bilayers and cations in agreement with experiments, which is presented in the next chapter. In this section, we show how the model captures the structure of phospholipid bilayers without ions, or with only counterions.

We chose phosphatidylcholine (PC), phosphatidylethanolamine (PE), and phosphatidylserine (PS) as representatives of the most common neutral and negatively charged lipids in the plasma membrane [van Meer and de Kroon, 2011, Marsh, 2013]. The Lipid14 [Dickson et al., 2014] model used for POPE and POPC, and the Lipid17 [Gould et al., 2018] model, already available from AmberTools [Salomon-Ferrer et al., 2013], were used as the starting point for embedding ECC. It was shown by Botan et al. [2015], Catte et al. [2016] that such a family of lipid models provides one of the most realistic descriptions of the head group order parameters of POPC and their response to ions when compared to other available lipid models.

In case of charged molecules, embedding ECC through a linear transformation of the partial charges in Eq. 2.3 is straightforward – applying ECC to a molecule with a formal charge -1 scales its total charge to -0.75. Note that the same scaling factor derived from the electronic dielectric constant of water was also applied to the charges of ECC-ions by Pluhařová et al. [2014], Kohagen et al. [2014, 2016], Martínek et al. [2018].

While the scaling factor of 0.75 is clearly justified for molecules with a non-zero total charge like ions or POPS, it is not *a priori* clear what factor shall be used for neutral or zwitterionic molecules, e.g. for POPE, and POPC. Unlike the total charge, the partial charges of particles forming molecules in simulations are not physical observables. There is a variety of schemes for assigning partial charges to particles in molecules [Hu et al., 2007]. The restrained electrostatic potential method (RESP) is, however, the most common method used in biomolecules [Bayly et al., 1993, Singh and Kollman, 1984, Dickson et al., 2014]. In practice, it is common that water molecules are included in the RESP calculations, and charges are subsequently refined to improve certain experimental observables. Although such tweaks do not affect the zero total charge for neutral molecules, it naturally follows from this fitting procedure that the effects of electronic polarizability may to some extent be present even in standard force fields [Bayly et al., 1993, Singh and Kollman, 1984, Jorgensen et al., 1996, Cerutti et al., 2013, Benavides et al., 2017]. We thus conclude that the scaling factor for partial charges in existing models of neutral molecules does not necessarily need to follow the relation 2.3. It is expected instead, that the scaling factor may adopt a slightly higher value than 0.75.

The ECC correction was applied on top of the Lipid14/Lipid17 models of POPC, POPE, and POPS by scaling the partial charges of all atoms except for the acyl tails, i.e., the polar parts in phospholipids, head group, glycerol backbone, and carbonyl regions. Such a choice was guided by the observed strength of interaction with cations. In contrast to the head group and the glycerol backbone atoms, the acyl chains do not come in direct contact with ions from the solution, and they are already highly optimized to provide a good description of the hydrophobic part of lipid bilayers Dickson et al. [2014], Ollila and Pabst [2016], Pluháčková et al. [2016]. In contrast to the acyl tails, the glycerol backbone and the head group regions of phospholipids require improvements in any available lipid model Botan et al. [2015], Bacle et al. [2018].

We found that the optimal value for the scaling factor of partial charges of neutral molecules from Lipid14 that yields accurate responses of the lipid head groups to the charges bound to the membrane is 0.8, which is indeed slightly higher than 0.75, i.e., the scaling factor for the ions in water. This value was found by comparing the results from the simulations with POPC to the experimental NMR data on the head group order parameter response to the bound charge. [Akutsu and Seelig, 1981, Altenbach and Seelig, 1984, Scherer and Seelig, 1989]

Although scaling of partial charges improved the head group order parameter response and ion binding affinity, it has at the same time deteriorated certain membrane properties; namely the area per lipid generally decreased, often below the experimental values. The decrease of the area per lipid is observed to arise from a reduced hydration of the lipid head group region as the polarity of the head group has decreased in overall after scaling of the charges.

We compensated for this artifact by reducing the effective radii of atoms with the scaled charges. This was explicitly done for POPC by changing the parameters σ in the Lennard-Jones potential in a similar way as was done previously for the ECC-ions in solution [Kohagen et al., 2014, 2016, Pluhařová et al., 2014]. Reducing the σ parameters of the affected atoms by a factor of $f_\sigma = 0.89$ restored the area per molecule to a value very close to experiment (Table 2.1). Such optimized parameters σ were then used for all ECC-lipids, i.e. also for ECC-POPE and ECC-POPS. In addition, the X-ray scattering form factors of POPC, POPE and POPS from simulations remained in a good agreement or even improved with these modifications (see Figs. 2.1, 2.2 and 2.3).

2.3.1 Structural parameters of model membranes with ECC-lipids: Agreement with experiments

We compared X-ray scattering form factors and NMR order parameters of bilayers in pure water without any ions (or only counter ions) from simulations and experiments as the first step in the assessment of the quality of the model. The experimental X-ray scattering form factors of a bilayer are well reproduced for all lipids employing the presented ECC-lipids model (see Figs. 2.1, 2.2 and 2.3).

The area per lipid is often used as a relatively simple structural parameter reporting on the bilayer properties and the packing of lipids. In experiments, modeling is used on top of the scattering factors to obtain it [Pan et al., 2014]. From simulations, this property is easily extracted. We compare the values from experiments and simulations in Table 2.1.

The area per lipid of POPC in simulation with ECC-lipids model is smaller by $\approx 1\text{Å}^2$ than the experimental value derived from the SDP model [Pan et al., 2014]. The values of the area per lipid of the ECC-POPC model vary slightly when simulated with different water models, however, they are still close to the experiment. [Melcr et al., 2018]

The experiments with POPE bilayers were performed only at higher temperatures than in the simulation [Rand and Parsegian, 1989, Rappolt et al., 2003], however, if we extrapolate the experimental values using the series in the work by Rappolt et al. [2003] (i.e., change of $\approx 1\text{Å}^2$ for each 5°C), the extrapolated estimate of the area per lipid from the simulation lays between the two distinct values from the experiments in Table 2.1.

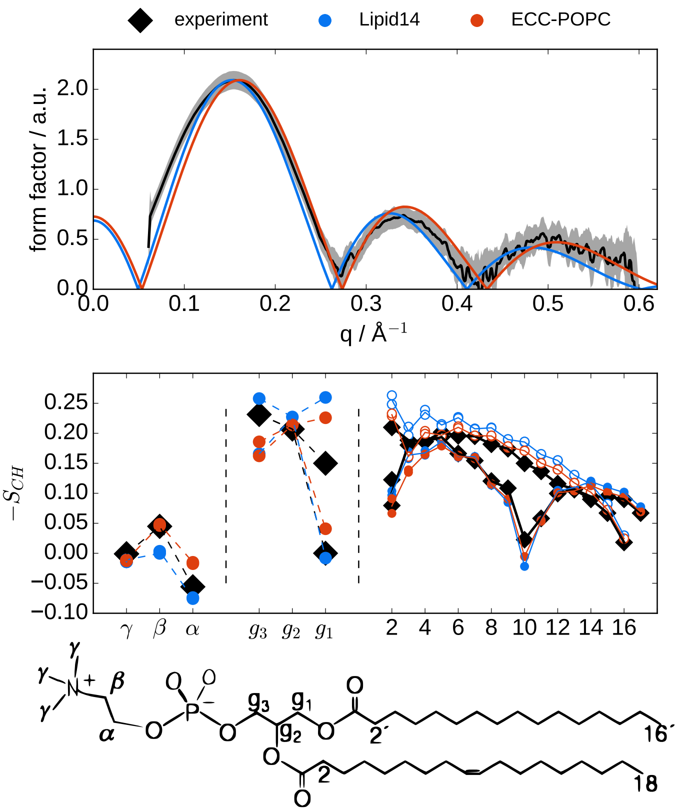

Figure 2.1: Top: X-ray scattering form factors from simulations with the Lipid14 [Dickson et al., 2014] and the ECC-POPC [Melcr et al., 2018] models compared with experiments [Kučerka et al., 2011] at 303 K. Middle: Order parameters of POPC head group, glycerol backbone and acyl chains from simulations with the Lipid14 and the ECC-POPC models compared with experiments [Ferreira et al., 2013] at 300 K. The size of the markers for the head group order parameters correspond to the error estimate ±0.02 for experiments [Botan et al., 2015, Ollila and Pabst, 2016], while the error estimate for simulations is ±0.005 (Bayesian estimate of 95% confidence interval [Jones et al., 2001–2018]). The size of the points for acyl chains are decreased by a factor of 3 to improve the clarity of the plot. Open/closed symbols are used for palmitoyl/oleoyl chains of POPC. Bottom: The chemical structure of POPC and the labeling of the carbon segments.

While the agreement between the scattering form factors from the simulation of a pure POPS bilayer and experiment are excellent (Fig. 2.3), there is a non-negligible difference between the values of the area per lipid in Table 2.1. Since both values are derived from the scattering form factors through modeling of the electron density of the bilayer, we cannot decide, which of the values is more reliable. In general, we can conclude that ECC-lipids reproduce the experimental structural parameters of the lipid bilayers with a comparable accuracy to existing state-of-the-art lipid models [Botan et al., 2015, Ollila and Pabst, 2016, Pluháčková et al., 2016].

The head group and acyl chain order parameters within ECC-lipids are in general in a good agreement with the experimental values as shown in Figs. 2.1, 2.2, and 2.3. The acyl chain order parameters in particular are almost all within the experimental error bars. The order parameters of the head groups are at an

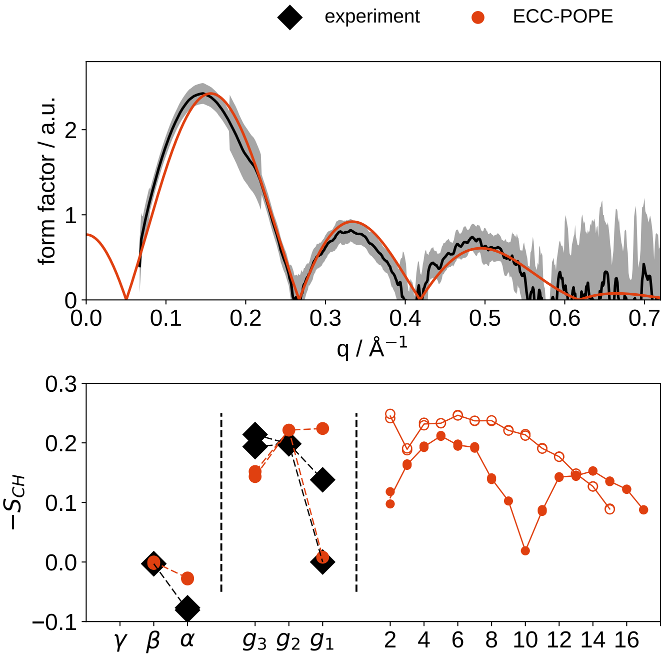

Figure 2.2: Top: X-ray scattering form factors from simulations with the ECC-lipids model of POPE compared with experiments Kučerka et al. [2011] at 313 K. Bottom: Order parameters of POPE head group, glycerol backbone and acyl chains from simulations with the ECC-lipids model of POPE compared with experiments by Gally et al. [1981] (order parameters of glycerol backbone, labeled *E. coli* membrane at 310 K,) and by Seelig and Gally [1976], Wohlgemuth et al. [1980] (order parameters α and β from DPPE at 341 K). The signs of the order parameters were not determined in the experiments, same signs as in POPC (Fig. 2.1) are assumed. Open/closed symbols are used for palmitoyl/oleoyl chains of POPE. The chemical structure of POPE is the same as for POPC in Fig. 2.1, but the methyl groups in choline (denoted with γ), which are substituted with hydrogen atoms in PE.

accuracy comparable to other currently available classical models of lipids [Botan et al., 2015, Catte et al., 2016, Pluháčková et al., 2016].

The head group order parameters α and β are highly relevant for this work, as they are being used in the electrometer concept (introduced in section 1.2). For POPC in pure water, the order parameter β agrees well with the experiment, while the order parameter α is somewhat lower. In the case of POPS, the situation is a bit more complicated compared to POPC as the order parameter α exhibits a notable forking (see Fig. 2.3). One of the order parameters of ECC-POPS, α_1, agrees well with the experiment, while the other, α_2, adopts a higher value underestimating the experimentally reported forking. There is only one order parameter β in POPS, which has a higher value closer to zero in the ECC-lipids model than in experiment. Such a feature suggests that the model overestimates the orientational freedom of its head group.

To our knowledge, there are no data on the order parameters in POPE. To get at least a rough estimate of the structure of PE head group from experiments, we can compare to either DPPE, which has palmitoyls in both acyl tails, and is measured at a different temperature 341 K [Seelig and Gally, 1976, Wohlgemuth

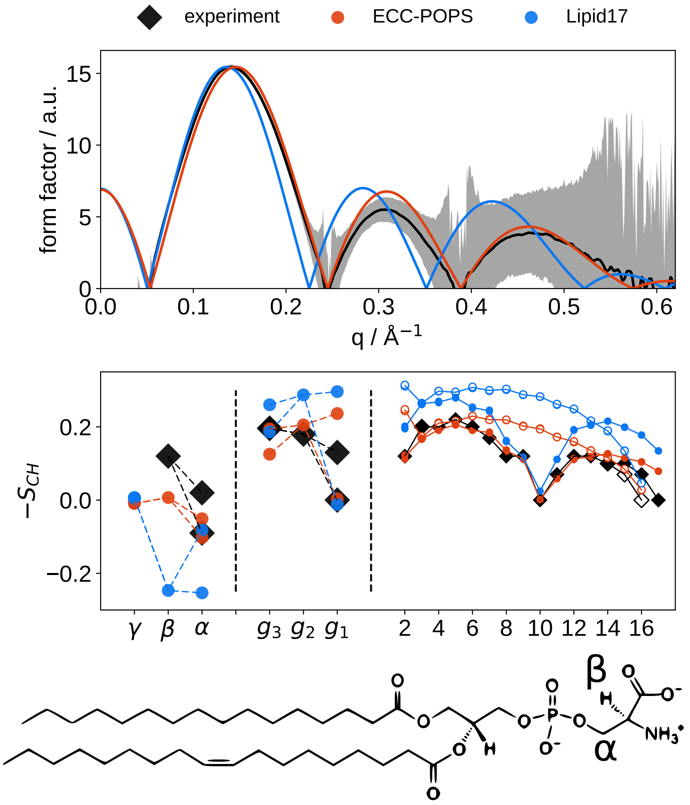

Figure 2.3: Top: X-ray scattering form factors from simulations with the Lipid17 [Gould et al., 2018] and the ECC-POPS models compared with experiments [Pan et al., 2014] at 298 K. Middle: Order parameters of POPS head group, glycerol backbone and acyl chains from simulations with the Lipid17 [Gould et al., 2018] and the ECC-POPS models compared with experiments at 298 K. [Bacle et al., 2018] Open/closed symbols are used for palmitoyl/oleoyl chains of POPS. Bottom: The chemical structure of POPS and the labeling of the carbon segments.

et al., 1980]; or a mixture of PE lipids from the membrane of *E. coli* at 310 K, [Gally et al., 1981]. Such data are used in Fig. 2.2 to provide estimates of the order parameters for related systems.

2.4 Modeling of transmembrane potential

The intracellular environment of cells contains a weak electrolytic solution of KCl, while there is a similarly weak solution of NaCl on the extracellular side. The concentrations of these salts, usually around 150 mM, are regulated and maintained out of equilibrium through specific channels and pumps to provide cellular functions and general homeostasis conditions [Bezanilla, 2008, Sten-Knudsen, 2002]. The unequal distribution of ions on either side of the membrane gives rise to a transmembrane potential. For instance, the concerted action of voltage-gated ion channels and pumps in neurons modulates their transmembrane potential providing a fast signal transduction through the axons [Sten-Knudsen, 2002, Storace et al., 2015, Sung et al., 2015]. The common magnitude of the transmembrane potential in cells is in the range of 10–100 mV. In experiment, the membrane potential can be measured using the patch clamp technique [Bezanilla, 2008] and

Table 2.1: Values of the area per lipid (APL) of POPC, POPE and POPS bilayers at temperatures T without additional ions.

POPC

model	APL / Å^2	T / K
Lipid14 POPC [Melcr et al., 2018]	65.1± 0.6	300
Lipid14 POPC [Dickson et al., 2014]	65.6± 0.5	303
ECC-POPC [Melcr et al., 2018]	63.2± 0.6	300
experiment (SDP model) [Kučerka et al., 2011]	64.3	303

POPE

model	APL / Å^2	T / K
ECC-POPE	56.7± 0.8	298
experiment [Rand and Parsegian, 1989]	56.6	310
experiment [Rappolt et al., 2003]	59–61	303–313

POPS

model	APL / Å^2	T / K
Lipid17 POPS	53.5± 0.8	298
ECC-POPS	60.3± 0.6	298
experiment (SDP model) [Pan et al., 2014]	62.3	298

the more modern voltage-sensitive fluorescent probes [Storace et al., 2015, Sung et al., 2015].

The transmembrane potential in simulations can be modeled by several methods. [Tieleman et al., 2001, Sin et al., 2015, Roux, 1997, Sachs et al., 2004a]. In particular, there are two approaches for the modeling of the membrane potential in atomistic molecular dynamics simulations – the constant electric field method [Roux, 1997, 2008, Gumbart et al., 2012], and the ion-imbalance method [Sachs et al., 2004a, Delemotte et al., 2008]. Both of these methods have been successfully used to study membrane electroporation or voltage-sensitive proteins [Vargas et al., 2012, Böckmann et al., 2008, Gumbart et al., 2012, Kutzner et al., 2011, Casciola et al., 2014]. These two practically independent developments were compared and connected together in our work [Melcr et al., 2016], where we prove them to be equivalent models of the transmembrane potential yielding indistinguishable results, at least for electrolytes formed by the same monovalent ions on both sides of the membrane. We used simulations in which we simultaneously applied both methods with the same magnitude but opposite polarity yielding zero transmembrane voltage in total to highlight possible artifacts. The comparison in Fig. 2.4 shows that such a setup is indistinguishable from simulations without voltage within the achievable accuracy. The electric field induced by the voltage exists exclusively in the hydrophobic region of the membrane, where it has an almost constant strength. This finding provides clues to understanding the evolutionary design of voltage-gated proteins. [Vargas et al., 2012] Moreover, the structure of the bilayer is preserved even at high voltages at the time scales of our simulations, unlike that of water at the interface with the hydrophobic core of the bilayer underlining its importance in electroporation. [Bu et al., 2017]

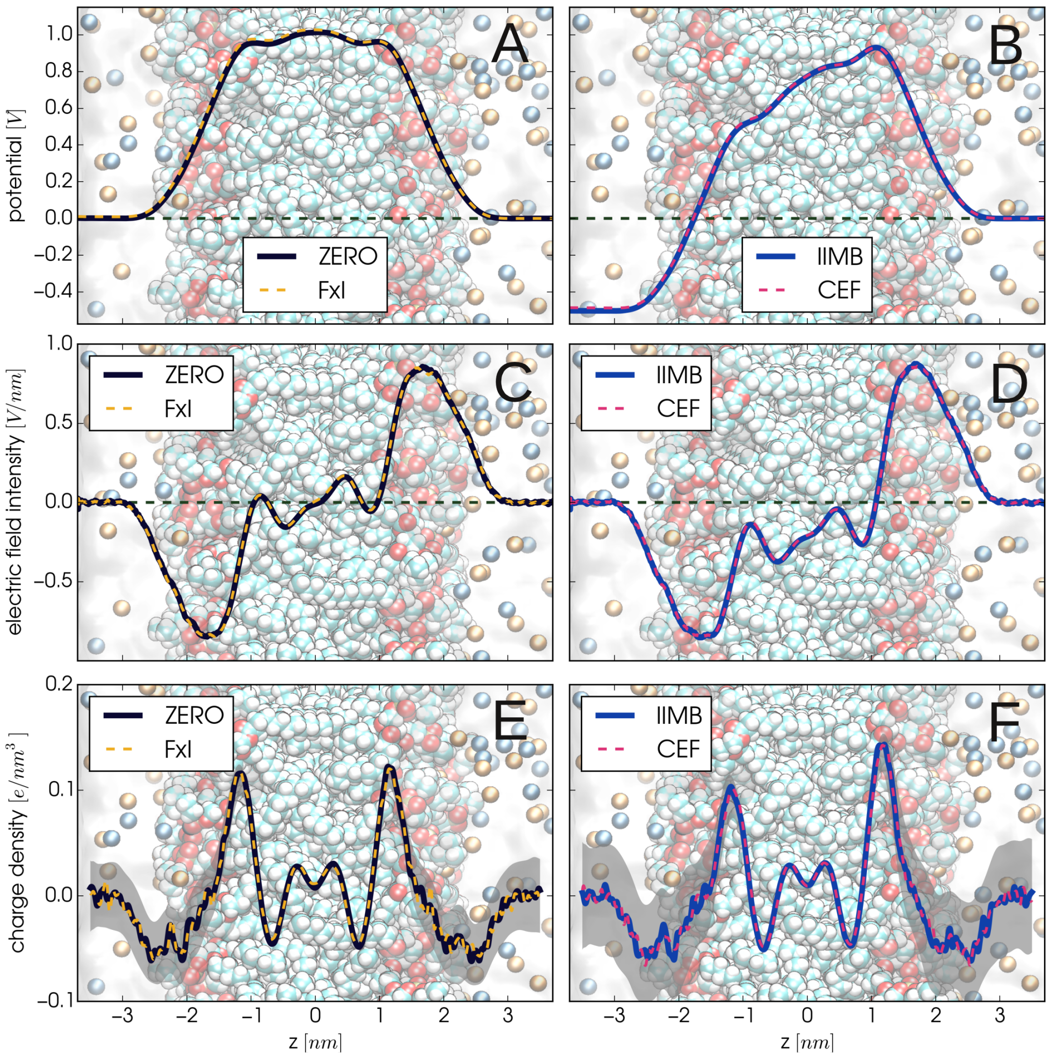

Figure 2.4: The transmembrane potential (A,B), the electric field intensity (C,D), and the charge density (E,F) profiles for simulations of a POPC bilayer with 150 mM concentration of KCl. ZERO stands for simulations without any applied voltage, IIMB stands for the ion imbalance method, CEF stands for the constant electric field method, and FxI denotes the special setup, in which the two methods are applied simultaneously. The gray area shows the standard error. The voltage drop across the membrane is 499 mV for IIMB and 486 mV for CEF with the error of about 7 mV.

3. Interactions of ions with phospholipid bilayers

Cellular membranes are surrounded by weak electrolytic solutions of KCl on the intracellular side, and of NaCl on the extracellular side. The biological relevance of these ions reaches from relatively simple osmotic effects to the complex processes in neural signalling. [Sten-Knudsen, 2002]

Calcium is an important cation in biology, which takes part in many signalling pathways and processes, e.g., triggering the release of neurotransmitters in neurons, allosteric activation of enzymes, regulating cardiac rhythm in the hearts, and contracting muscles. [Wang et al., 2000, Michalak et al., 2002, Glancy et al., 2013, Chouhan et al., 2012, Berridge et al., 2003, Clapham, 2007, Annunziata and D'Azzo, 2013, Timr et al., 2018] The interactions of Ca^{2+} with phospholipid membranes has recently received attention from both experiments and simulations [Melcrová et al., 2016, Javanainen et al., 2017, Catte et al., 2016, Melcr et al., 2018, Magarkar et al., 2017, Fink et al., 2017, Ye et al., 2018].

In this chapter, we will provide a detailed insight into the interactions of these ions with neutral and negatively charged model membranes, namely with a POPC bilayer and with a negatively charged bilayer with the composition of 5 POPC:1 POPS. We employ our newly developed models of ions and phospholipids, i.e., ECC-ions [Martínek et al., 2018, Kohagen et al., 2016, Pluhařová et al., 2014] and ECC-lipids [Melcr et al., 2018], which provide a major improvement over any state-of-the-art model of ions or lipids in terms of lipid-ion interactions.

First, we summarize the literature knowledge on the interactions of ions with membranes in experiments and simulations. Then, we demonstrate the accuracy of the newly developed lipid models from ECC-lipids by showing the response of the head group order parameters to a membrane-bound charge. At last, we will provide detailed insight into the binding of cations to the neutral and negatively charged bilayers. We put extra emphasis on the interactions with Ca^{2+}, for which we present the first simulation results that are in *quantitative* agreement with experiments. [Altenbach and Seelig, 1984, Catte et al., 2016, Bacle et al., 2018, Melcr et al., 2018]

3.1 Binding of cations to phospholipid bilayers and lipid electrometer concept from experiments and simulations

The response of the lipid head group order parameters to a given amount of bound charge in bilayers was calibrated using monovalently charged surfactants in [Scherer and Seelig, 1989, Akutsu and Seelig, 1981, Altenbach and Seelig, 1984]. After such a calibration, binding affinities of free cations can be estimated from the measured head group order parameter changes. [Scherer and Seelig, 1989] This forms the lipid electrometer concept (introduced in section 1.2), which can be used to directly compare experimental measurements with MD simulations. We performed such a comparison for both neutral and negatively charged membranes in NaCl and $CaCl_2$ aqueous solutions using a large set of MD simulations produced within NMRlipids open collaboration platform [Miettinen and Ollila, 2018]. It was concluded that the binding affinities of cations are overestimated in almost all models studied in [Catte et al., 2016] (Fig. 3.1) and in [Bacle et al., 2018].

For neutral POPC bilayers, the small PC head group order parameter response to NaCl from the experiments by Seelig et al. [1987] is captured by only a few models, namely Lipid14 [Dickson et al., 2014], Orange [1] and CHARMM36 [Klauda et al., 2010]. However, the experimentally measured head group order parameter response to $CaCl_2$ is not reproduced quantitatively by the models. [Catte et al., 2016] In addition, none of the employed models in that study reproduces the order parameters without any salt concentration within experimental error, indicating structural inaccuracies of varying severity in all of them [Botan et al., 2015]. In summary, all models of a PC bilayer examined in [Catte et al., 2016] overestimate the response of head group order parameters and/or binding affinity of $CaCl_2$ to such bilayers.

Similar conclusions to those from neutral POPC bilayers are also reached for negatively charged membranes containing POPS [Bacle et al., 2018]. The structure of a POPS bilayer with only Na^+ counterions is not captured within the experimental error by any of the studied models. However, the small response of the order parameters of PC and PS head groups to increasing concentrations of NaCl in a mixed bilayer with the composition 5 PC:1 PS is captured by a few, namely Lipid17 [Gould et al., 2018], and less well in MacRog [Maciejewski et al., 2014].

Interestingly, the response to $CaCl_2$ is overestimated by all employed models but one, CHARMM36 obtained from `http://charmm-gui.org/` [Jo et al., 2008, Lee et al., 2016], which contains an ad hoc correction for the observed excessive binding of Ca^{2+} to PC and PS similar to the correction for Na^+ [Venable et al., 2013]. With such a model, the response of the head group order parameters of PC to increasing concentrations of $CaCl_2$ in a mixed negatively charged bilayer is significantly reduced by the employed correction for Ca^{2+}, even below the response measured experimentally. Hence, it is the only model in the study, which underestimates the response of the lipid electrometer for the negatively charged membrane. This is in stark contrast to the results from the neutral POPC bilayer in [Catte et al., 2016], where the ad hoc repulsive correction for Ca^{2+} was not yet present.

In order to distinguish, whether the observed discrepancy of the head group order parameter changes between simulations and experiments arises from an incorrect sensitivity of the head group or from an excessive binding of cations to the phospholipid bilayers, we performed simulations of a neutral POPC bilayer with varying amounts of a cationic surfactant dihexadecyldimethylammonium, as was measured in the experimental work by Scherer and Seelig [1989]. The amount of bound charge per lipid in such systems is given simply by the molar fraction of the cationic surfactants, as essentially all of the surfactants segregate to the lipid bilayers due to the two long hydrophobic tails. The NMR measurements of such systems can be used to validate the sensitivity of lipid head group order parameters (i.e., the coefficient m_i in Equation 1.2) to the amount of bound

---

[1] See supplementary information in [Catte et al., 2016] for further information about the model Orange.

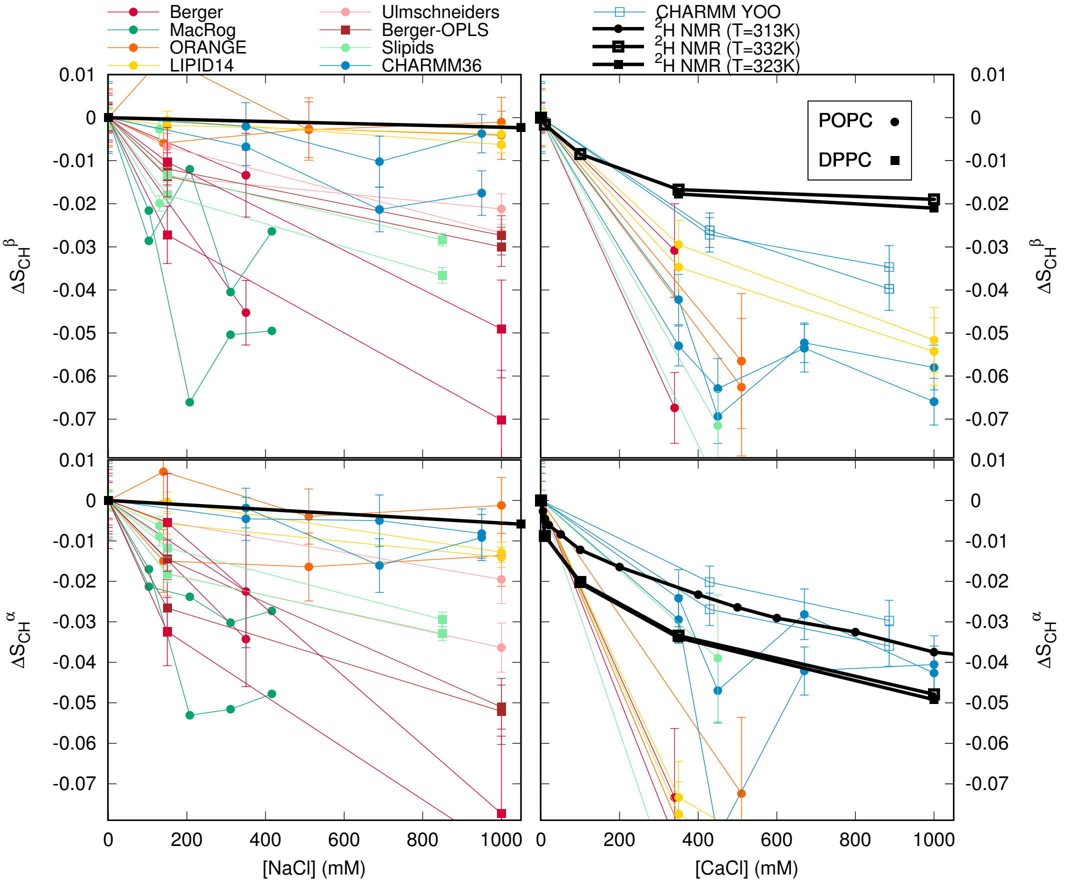

Figure 3.1: Changes of the head group order parameters β (top row) and α (bottom row) to increasing concentrations of NaCl (left column) and CaCl$_2$ (right column) Results from experiments (DPPC from Ref. [Akutsu and Seelig, 1981], POPC from Ref. [Altenbach and Seelig, 1984]) are compared with simulations with different force fields [Miettinen and Ollila, 2018, Catte et al., 2016]. Note that none of the employed models in this figure reproduces the order parameters without any salt concentration within experimental error, indicating structural inaccuracies of varying severity in all of them [Botan et al., 2015].

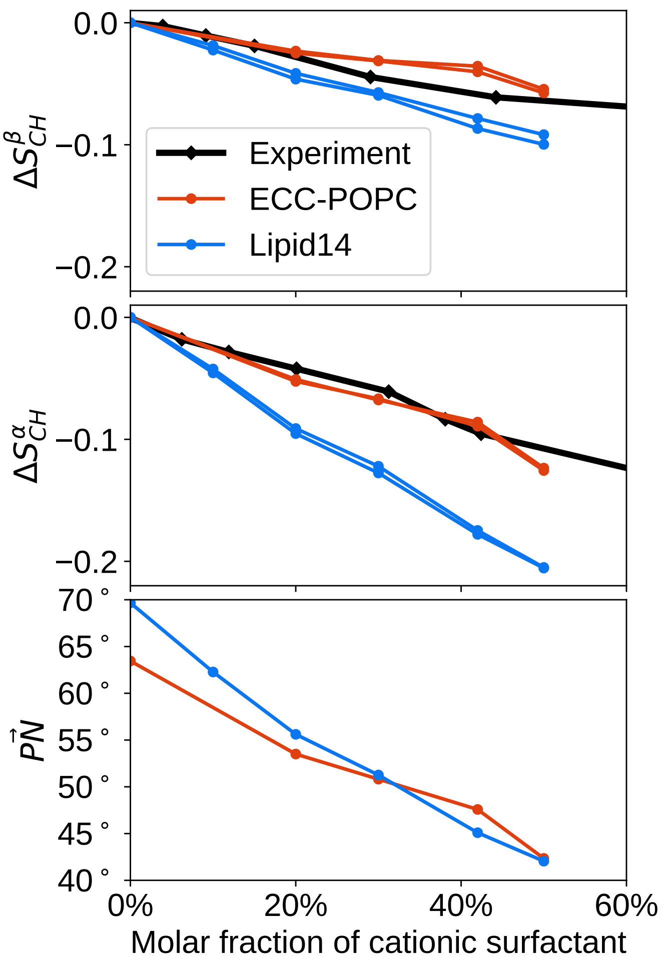

Figure 3.2: Changes of the head group order parameters α, β and P-N vector orientation as a function of the molar fraction of a cationic surfactant dihexadecyldimethylammonium in a POPC bilayer from simulations and experiments [Scherer and Seelig, 1989] at 313 K.

charge in simulations.

The changes of the head group order parameters in a POPC bilayer with an increasing amount of the cationic surfactant from simulations and experiments [Scherer and Seelig, 1989] are shown in Fig. 3.2. In line with Equation 1.2, experiments as well as both MD simulation models show an approximately linear decrease of the head group order parameters α and β. The slope of the response of the order parameters from the simulation with the ECC-POPC model is in a very good agreement with the experiments, whereas the slope from the simulations with Lipid14 is too steep. This shows that the overestimated response in the work [Catte et al., 2016] arises at least in part from an excessively sensitive response of the head group.

The increasing amount of the cationic surfactant in the bilayer also affects the P-N vector, which is defined as the angle between the connector of the phosphorus and nitrogen atoms and the membrane normal. Similarly to the order parameters, there is a linear dependence on the amount of the cationic surfactant as shown in Fig. 3.2. Although the structure of the ECC-POPC model without any ions does not agree with NMR experiments within error bars, such a model reproduces

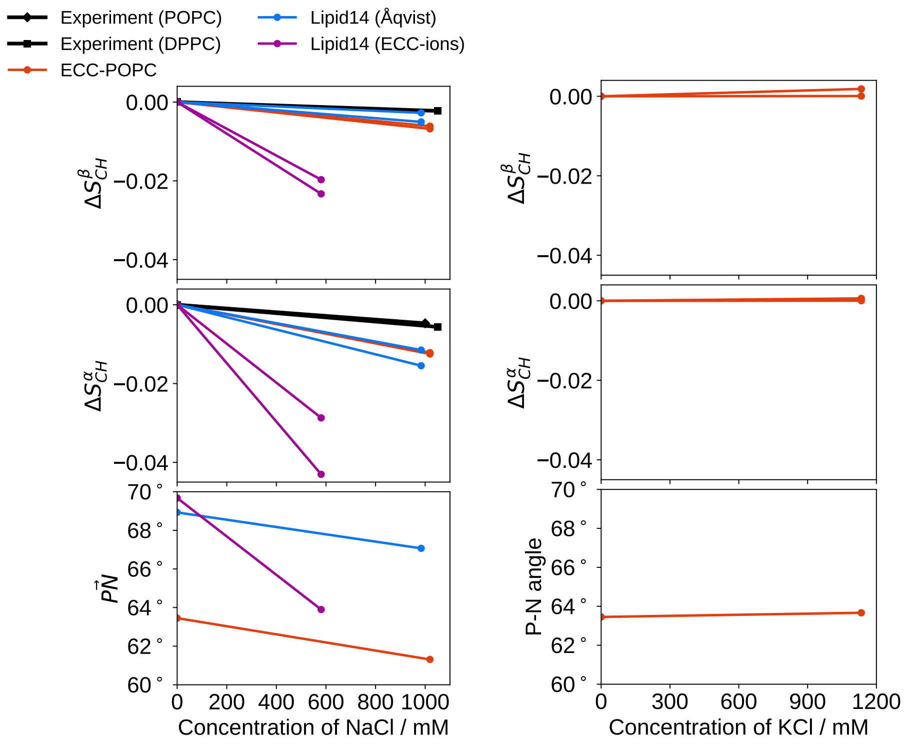

Figure 3.3: Changes of head group order parameters α and β and P-N vector orientation in a POPC bilayer as a function of NaCl (left) and KCl (right) concentration in bulk (C_{ion}) from simulations with different force fields at 313 K together with experimental data for DPPC (323 K) [Akutsu and Seelig, 1981] and POPC (313 K) [Altenbach and Seelig, 1984]. Simulation data with Lipid14 and Åqvist ion parameters at 298 K are taken directly from Refs. [Girych and Ollila, 2015a,b].

well the changes of the order parameters. It follows from these observations that using this model we can write an approximate relation between the changes of the order parameters and the P-N vector mean orientation. For the change of the order parameter α, ΔS^{α}, we arrive at

$$\Delta \vec{PN} = (186^\circ \pm 9^\circ) \cdot \Delta S^{\alpha}. \tag{3.1}$$

This relation can be used to estimate the change of the P-N vector as a mean orientation of the head group from experimental measurements of the change of the order parameter α in POPC.

3.2 Interactions of neutral and negatively charged phospholipid membranes with Na^+ and K^+ cations

The binding of Na^+ cations to phospholipid bilayers is not generally agreed on between simulations [Böckmann et al., 2003, Sachs et al., 2004b, Berkowitz et al., 2006, Cordomí et al., 2009] and experiments [Cevc, 1990, Tocanne and Teissié,

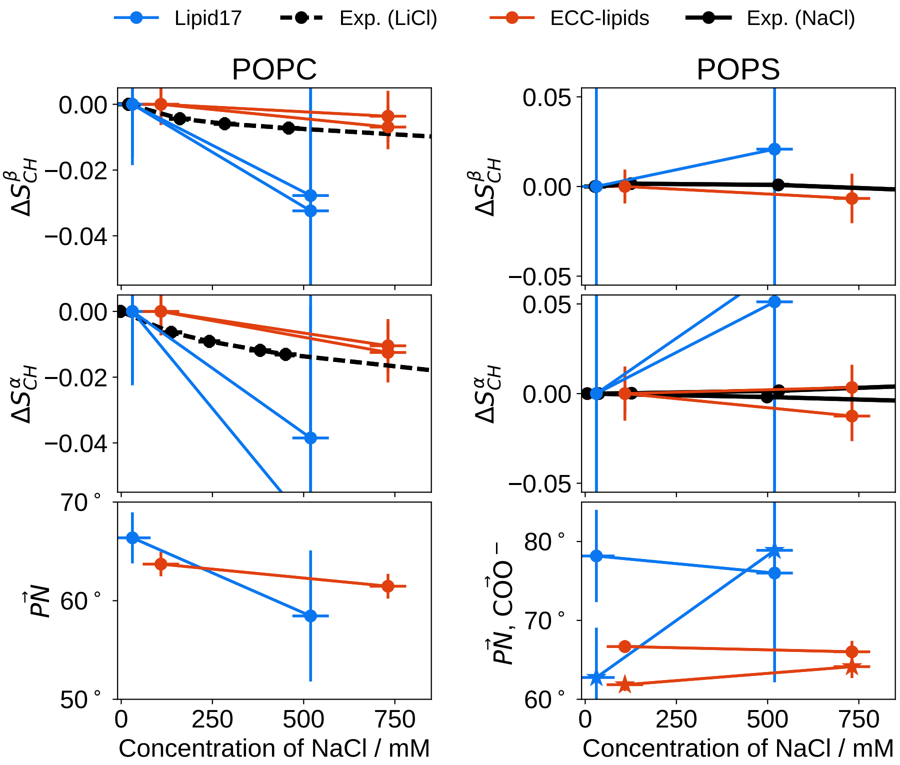

Figure 3.4: Changes of the head group order parameters α, β and the orientations of the carboxylate group and the P-N vector of POPC (left) and POPS (right) phospholipids in a POPC:POPS 5:1 bilayer as a function of NaCl concentration in bulk (C_{ion}) from simulations with different force fields at 298 K. Because data with NaCl are not available for POPC, we show experimental data for LiCl (dashed line, left) as an upper bound for the magnitude of the response to NaCl, which has a lower affinity to phospholipid bilayers compared to LiCl [Roux and Bloom, 1990]. The orientation of the COO$^-$ group is defined as the connector from the β carbon to the carbon in COO$^-$ (stars, bottom right).

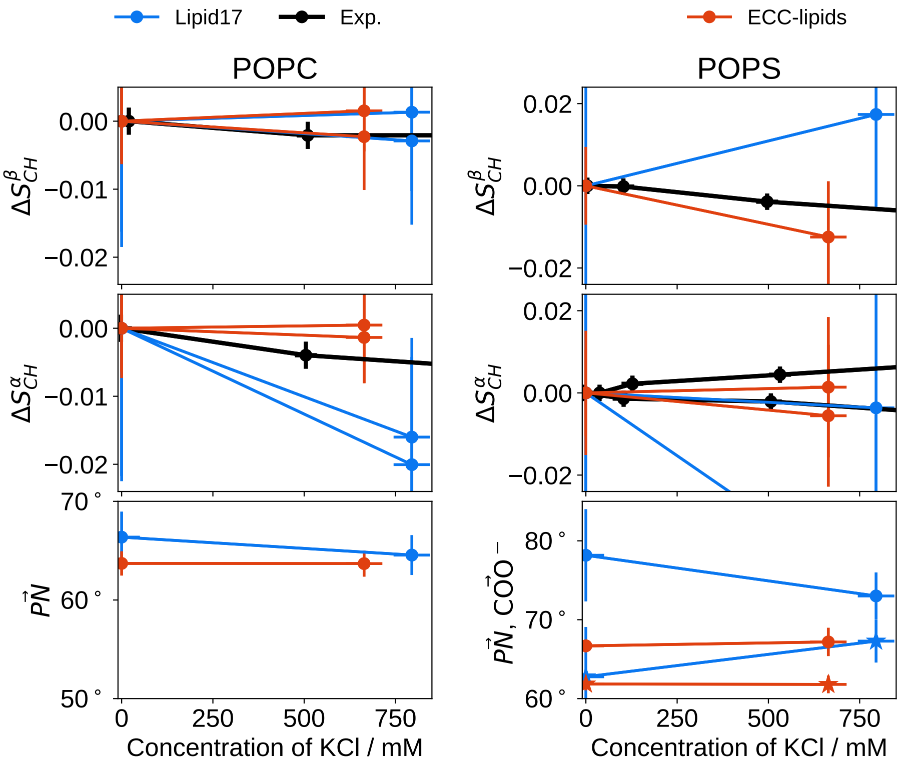

Figure 3.5: Changes of the head group order parameters α, β and the orientations of the carboxylate group and the P-N vector of POPC (left) and POPS (right) phospholipids in a POPC:POPS 5:1 bilayer as a function of KCl concentration in bulk (C_{ion}) from simulations with different force fields and experiments at 298 K. [Roux and Bloom, 1990] The orientation of the COO$^-$ group is defined as the connector from the β carbon to the carbon in COO$^-$ (stars, bottom right).

1990, Hauser et al., 1976, Herbette et al., 1984, Uhríková et al., 2008]. We attempted to find a model, which would successfully interpret the experiments on binding of Na^+ to neutral and negatively charged phospholipid bilayers [Akutsu and Seelig, 1981, Roux and Bloom, 1990] in our works [Catte et al., 2016, Bacle et al., 2018]. After testing the currently available force fields for phospholipids, we concluded that the interactions are generally overestimated in magnitude in almost all models but Lipid14 (PC) [Dickson et al., 2014], resp. Lipid17 (PS) [Gould et al., 2018]. This model yields a semi-quantitative agreement with the experimentally measured small changes of the order parameters when used with the model of ions by Åqvist [1990] (Fig. 3.1). However, when used with a more accurate model of ions by Pluhařová et al. [2014], Martínek et al. [2018], the model overestimates the binding affinity of Na^+ measured with lipid electrometer concept in Fig. 3.3. [Melcr et al., 2018] In total, these results suggest that improvements in the lipid parameters are required for more accurate interactions even with monovalent cations. [Catte et al., 2016, Melcr et al., 2018, Bacle et al., 2018]

Generally improved behaviour of the POPC and POPS head group order parameters with NaCl or KCl concentrations was achieved through the combination of models ECC-lipids [Melcr et al., 2018] and ECC-ions [Martínek et al., 2018, Kohagen et al., 2016, Pluhařová et al., 2014]. Simulations with these models reveal a good agreement with the NMR experiments for both neutral and negatively charged membranes. The results are plotted for NaCl in Figs. 3.3 and 3.4, and for KCl in Figs. 3.3 and 3.5.

The interaction with K^+, which binds very weakly to both neutral and negatively charged membranes, renders a qualitatively different response of the order parameter S^β in POPS in the mixed negatively charged bilayers compared to the neutral bilayers. While the order parameter S^β increases for both Na^+ and Ca^{2+}, it decreases in the presence of K^+. However, no model studied in [Bacle et al., 2018] describes the behaviour of a PS head group correctly enough to reveal this effect. In contrast, ECC-lipids with ECC-ions capture the different response of the order parameters S^β, S^{α_1} and S^{α_2} in POPS to various salts accurately. Such a detailed description of the changes of the structural parameters demonstrates that including electronic polarization improves the description of the interactions even for very weakly binding cations like K^+.

The difference between the affinities of Na^+ and K^+ to neutral and negatively charged membranes can be described by their relative surface excesses with respect to water, Γ^w_{ion}, which are shown in the plots of the density profiles of the ions in Figs. 3.6 (neutral bilayer) and 3.7 (negatively charged bilayer). Such a quantity compares the adsorption of ions to the adsorption of water molecules at an interface without the necessity of defining a Gibbs dividing surface. [Melcr et al., 2018, Chattoraj and Birdi, 1984] While K^+ maintains negative values of Γ^w_K even for the negatively charged bilayer, the value of Γ^w_{Na} for Na^+ changes from negative to positive in a neutral POPC bilayer versus in a negatively charged bilayer with the composition 5 PC:1 PS. Interestingly, this value is slightly decreased in the presence of an additional NaCl concentration adding also Cl^- anions, which are not present in the system when only counterions are used (bottom resp. top plot in Fig. 3.7). The interaction of a neutral POPC bilayer with NaCl is discussed in a greater detail in our publication [Melcr et al., 2018].

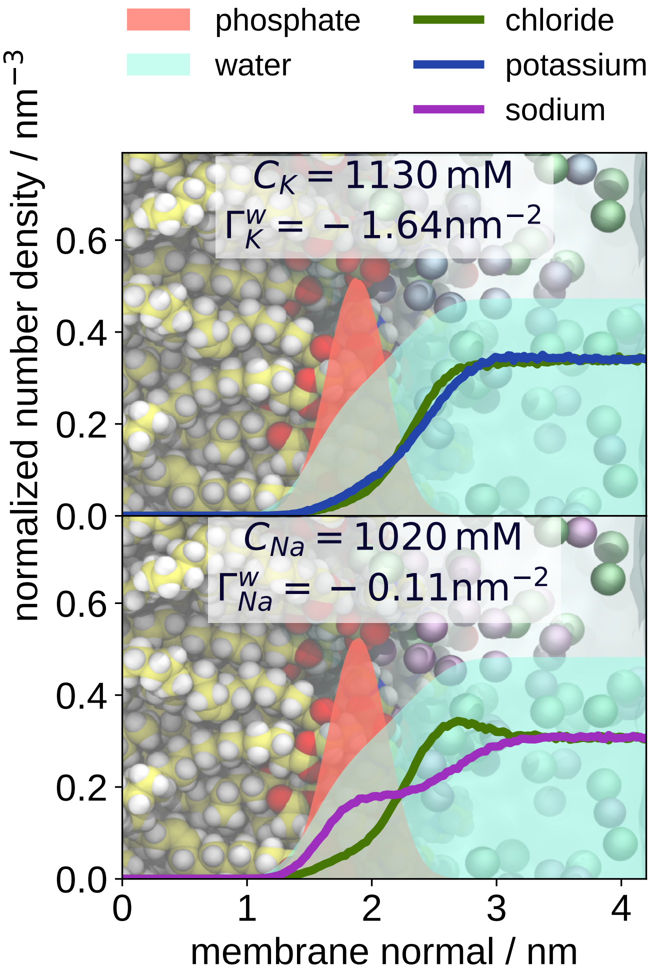

Figure 3.6: Number density profiles of K^+, Na^+ and Cl^- along the membrane normal axis from the simulations with the neutral POPC bilayer using ECC-lipids and ECC-ions. In order to visualize the density profiles with a scale comparable to the profile of Ca^{2+} in Fig. 3.10, the density profiles of Cl^-, K^+ and Na^+ ions are divided by 2, and the density profiles of phosphate groups and water are divided by 5 and 200, respectively. Both simulations have the same molar fractions of NaCl resp. KCl in water, C'_{ion}=1000 mM.

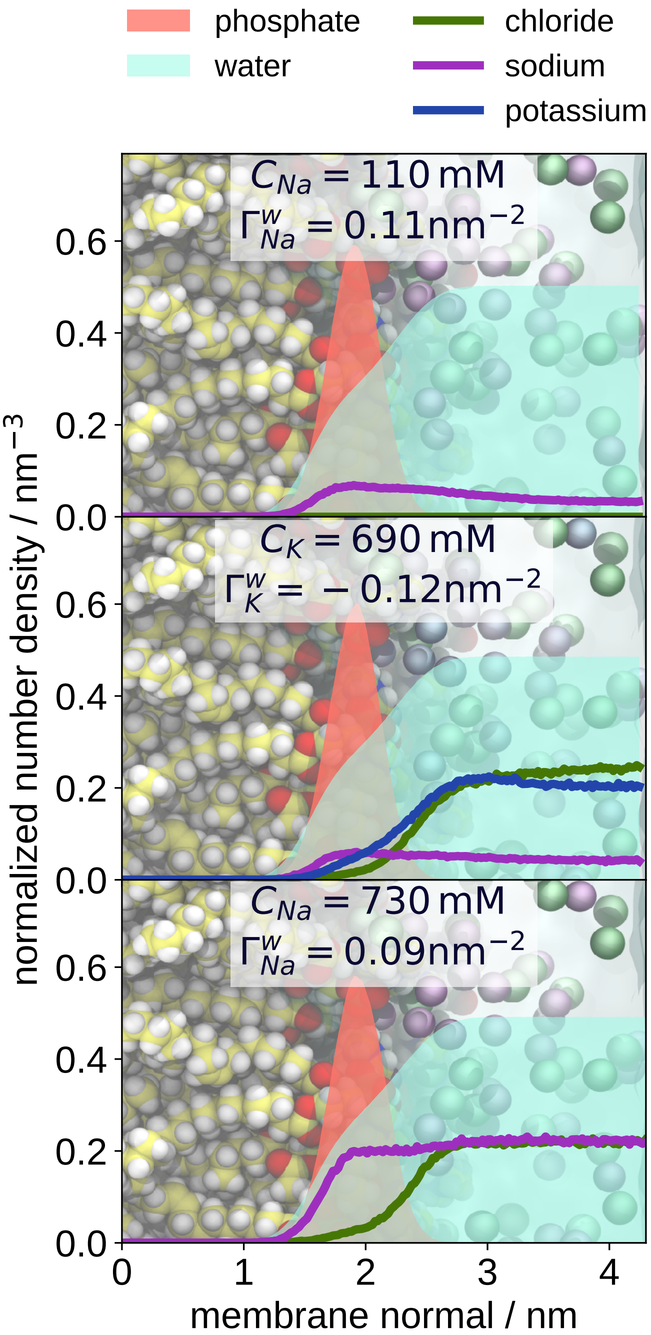

Figure 3.7: Number density profiles of K^+, Na^+ and Cl^- along the membrane normal axis for the negatively charged membranes with the composition of 5 PC:1 PS using ECC-lipids and ECC-ions. The top profile shows the simulation without any additional salt concentration, i.e., only with Na^+ counterions. The middle profile shows the simulation with an additional KCl concentration and Na^+ counterions. The bottom profile shows the simulation with an additional NaCl concentration and Na^+ counterions, which are not distinguished from the added salt. In order to visualize the density profiles with a scale comparable to the profile of Ca^{2+} in Fig. 3.10, the density profiles of Cl^-, K^+ and Na^+ ions are divided by 2, and the density profiles of phosphate groups and water are divided by 5 and 200, respectively.

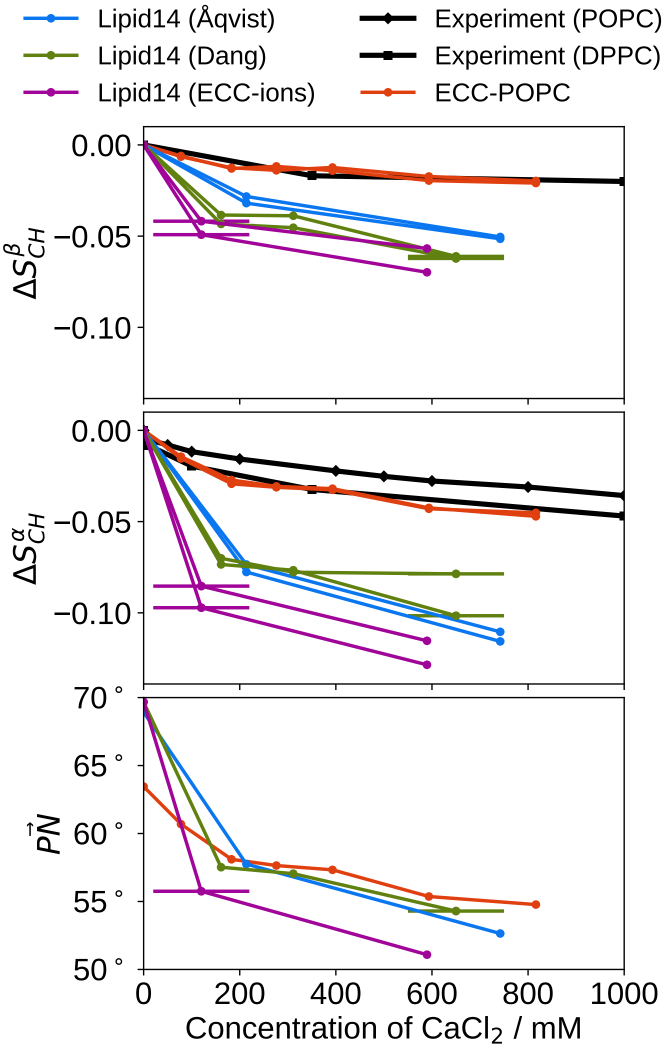

Figure 3.8: Changes of the head group order parameters and P-N vector orientation of a POPC bilayer as a function of the CaCl$_2$ concentration in bulk (C_{ion}) from simulations at 313 K together with experimental data (DPPC (323 K) [Akutsu and Seelig, 1981] and POPC (313 K) [Altenbach and Seelig, 1984]). The error estimate for bulk concentrations is approximately 10 mM. The order of magnitude larger error in the simulation with Lipid14 and ECC-ions is due to unconverged bulk densities limited by the simulation box. Simulation data with Lipid14 and Åqvist ion parameters at 298 K are taken directly from Refs. [Girych and Ollila, 2015a,c, 2016].

3.3 Interactions of neutral and negatively charged phospholipid membranes with Ca^{2+} cations

Electronic polarization is a non-negligible contribution to the interactions of calcium even in simple aqueous solutions of CaCl$_2$ [Martínek et al., 2018, Kohagen et al., 2016, Pluhařová et al., 2014]. In this section, we will show the results from simulations of neutral and negatively charged phospholipid bilayers at vary-

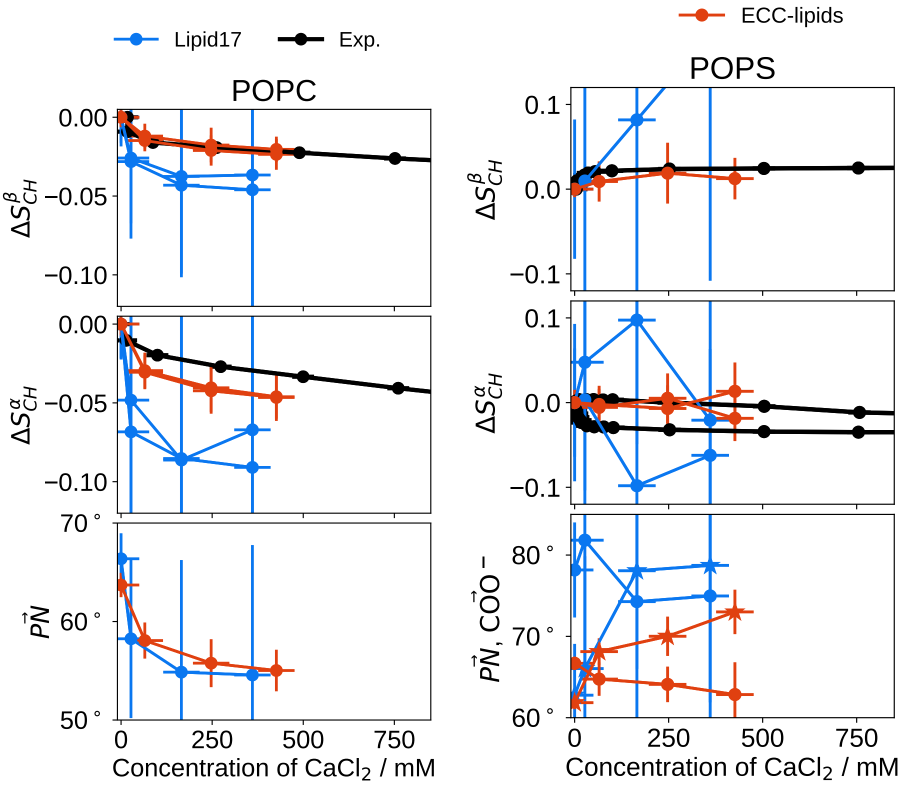

Figure 3.9: Changes of the head group order parameters α, β and the orientations of the carboxylate group and the P-N vector of POPC (left) and POPS (right) phospholipids in a POPC:POPS 5:1 bilayer as a function of CaCl$_2$ concentration in bulk (C_{ion}) from simulations with different force fields and experiments at 298 K. [Roux and Bloom, 1990] The orientation of the COO$^-$ group is defined as the connector from the β carbon to the carbon in COO$^-$ (stars, bottom right).

ing $CaCl_2$ concentrations using the recently developed models ECC-lipids and ECC-ions [Melcr et al., 2018, Martínek et al., 2018], which implicitly include the effects of electronic polarization through electronic continuum correction [Leontyev and Stuchebrukhov, 2011]. Validated with the concept of a lipid electrometer in section 3.1, these implicitly polarizable models yield accurate description of the interaction of Ca^{2+} with both neutral and negatively charged phospholipids.

The changes of the head group order parameters S^{α} and S^{β} from simulations and experiments are shown in Fig. 3.8 for a neutral POPC bilayer, and in Fig. 3.9 for a negatively charged bilayer with the composition 5 PC:1 PS. For a direct comparison and a connection to our works [Catte et al., 2016, Bacle et al., 2018], we show simulation results from ECC-lipids and also from Lipid17 [Gould et al., 2018]. This also highlights the improvements in ECC-lipids over Lipid17 arising from the electronic polarization. The effect is probably the most striking for POPS, for which also the structure of a pure POPS bilayer with only counterions is dramatically improved with the augmentation.

Increasing concentrations of $CaCl_2$ induce a systematic decrease of the order parameters S^{α} and S^{β} in POPC. Although the total magnitude of the response of the PC head group order parameters is only slightly higher in the negatively charged bilayers than in the neutral bilayers, the shape of the changes in the latter shows a steeper onset at low concentrations. This is apparently due to the presence of POPS, which has a higher affinity to Ca^{2+} compared to POPC. ECC-lipids is the first model, which achieves a *quantitative* agreement with the changes induced by $CaCl_2$ in experiments.

The increase in the amount of bound calcium cations from pure POPC to the mixed negatively charged bilayer containing POPS is well demonstrated using the relative surface excess, Γ^{w}_{Ca}, summarized in Table 3.1. Distributions of Ca^{2+}, Na^{+} counterions and also Cl^{-} are plotted in Fig. 3.10 for the neutral POPC bilayer, and in Fig. 3.11 for the negatively charged bilayer. In contrast to KCl or added concentrations of NaCl, Na^{+} counterions are substituted with Ca^{2+} even at low concentrations of $CaCl_2$. The increasing concentration of $CaCl_2$ and, hence, a higher amount of bound Ca^{2+} also attracts Cl^{-} anions to the bilayer as can be seen from its growing density at the interface.

The density profiles of ions suggest that the dominant contribution to the binding of Ca^{2+} to phospholipid bilayers comes from the interactions with the phosphate groups in both POPC and POPS. This is also reflected in the shift of the mean orientation of the COO^{-} group from 62° to 73° (420 mM $CaCl_2$) which was measured as the connector of the carbon atoms forming the bond between the group and the β-carbon of the phospholipid. The interactions of the carboxylate group in PS with calcium and other phosphate groups shed light into the qualitatively different response of the head group order parameters α and β in PS compared to PC (see Figs. 3.8 and 3.9). We find that the complex response of the head group order parameters of POPS is affected by the conformational changes of the carboxylate group, which is attracted more towards the phosphate region, where the calcium cations dominantly bind. In line with the experimental work by Browning and Seelig [1980], this is also very likely the reason, why the magnitude of the P-N vector change in POPS is diminished compared to POPC, which is not restrained by an additional cation binding group like COO^{-} in POPS.

Further details about the interactions of Ca^{2+} with various moieties in POPC

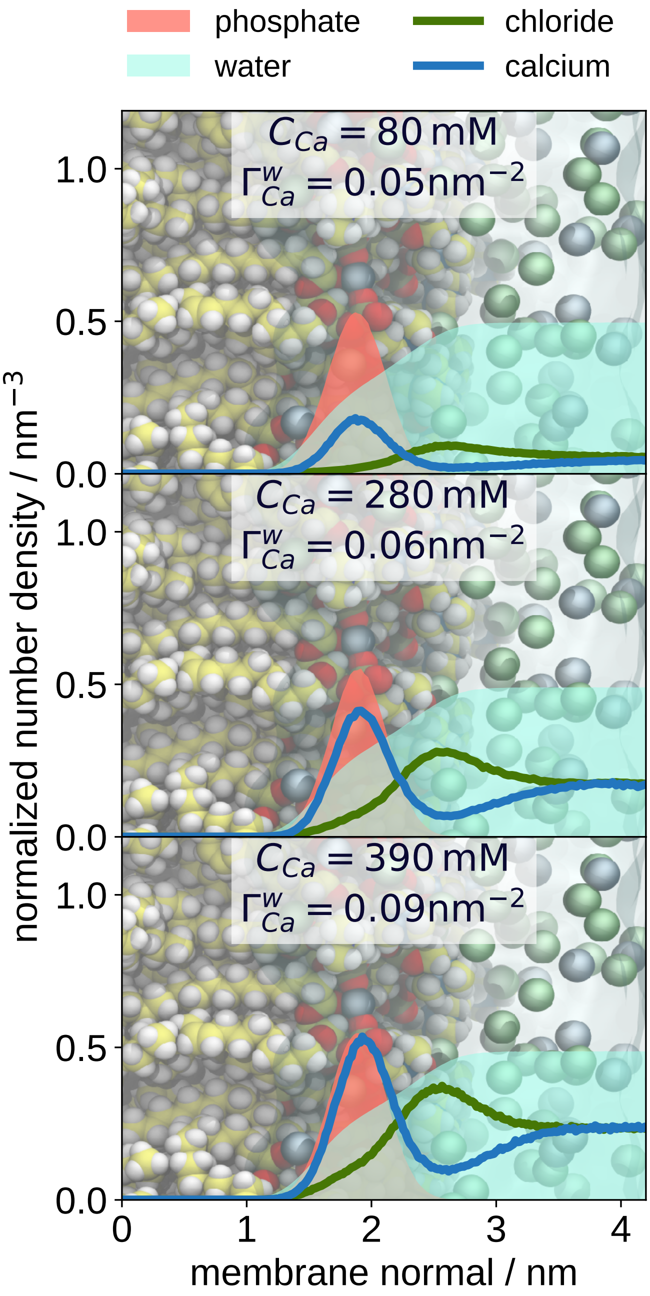

Figure 3.10: Number density profiles of Ca^{2+} and Cl^{-} along the normal of the neutral POPC bilayers starting at the centre for different concentrations of $CaCl_2$ from simulations with ECC-lipids. In order to visualize the density profiles with a scale comparable to the profile of Ca^{2+}, the density profiles of Cl^{-} ions are divided by 2, and the density profiles of phosphate groups and water are divided by 5 and 200, respectively.

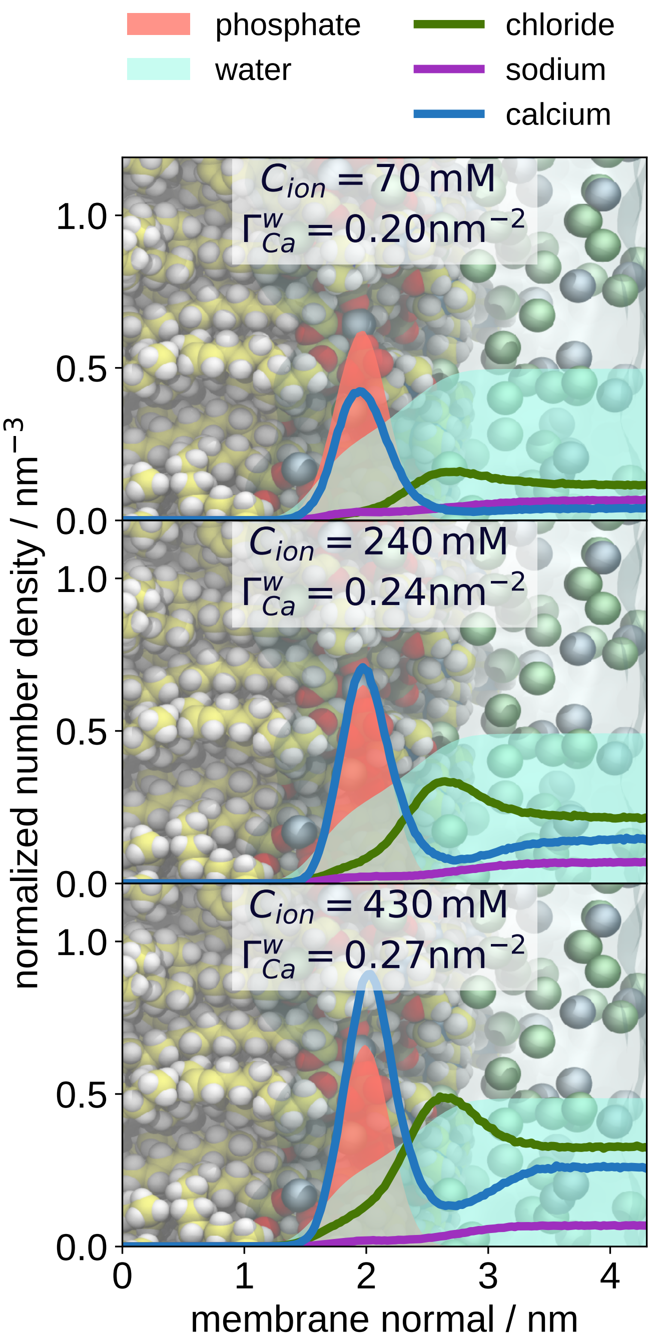

Figure 3.11: Number density profiles of Ca^{2+}, Na^{+} and Cl^{-} along the normal of the membrane starting at the centre for the negatively charged membrane with the composition 5 PC:1 PS at various bulk concentrations of $CaCl_2$ from simulations with ECC-lipids. All profiles contain Na^{+} counterions and an additional concentration of $CaCl_2$. In order to visualize the density profiles with a scale comparable to the profile of Ca^{2+}, the density profiles of Cl^{-} ions are divided by 2, and the density profiles of phosphate groups and water are divided by 5 and 200, respectively.

Table 3.1: Bulk concentrations, C_{Ca}, and molar fractions, C'_{Ca}, of Ca^{2+}; relative surface excess of calcium with respect to water ($\Gamma_{Ca}^{\text{water}}$); and percentages of the population of bound Ca^{2+} to various moieties in a neutral membrane composed of POPC and in a negatively charged membrane with the composition 5 PC:1 PS.

	5 POPC:1 POPS	POPC
C_{Ca} / mM	240 ± 10	280 ± 10
C'_{Ca} / mM	400 ± 10	350 ± 10
$\Gamma_{Ca}^{\text{water}}$ / nm^{-2}	0.24 ± 0.01	0.06 ± 0.01
interacting moiety	percentage of bound Ca^{2+}	
PC	59	100
PO_4 in PC	41	67
carbonyls in PC	<1	1
PS	8	
PO_4 in PS	2	
COO^- in PS	4	
carbonyls in PS	<1	
both PC and PS	33	

or POPS were obtained by counting contacts between the cations and the oxygen atoms of the lipids similarly as was done in Melcr et al. [2018]. The threshold for counting a contact was set to 0.3 nm, which encompasses the first peak of the radial distribution function between the cations and the oxygen atoms of the lipids.

The percentages of the populations of membrane-bound calcium cations for various membrane moieties are summarized in Table 3.1. Even though the negatively charged membrane contains only 18% of POPS, approximately 41% of the total population of bound calcium cations is in contact with PS lipids with 8% bound only to them. This corroborates the intrinsically higher affinity of PS lipids to calcium cations compared to neutral PC lipids. POPC interacts with the calcium cations almost entirely through its phosphate group in both neutral and negatively charged membranes, which is visualized using probability density isocontours in Fig. 3.12. Interactions of Ca^{2+} with carbonyl groups are also present, however, they are always accompanied by interactions with phosphate groups.

Relative probabilities of Ca^{2+} complexes with a certain number of lipids are presented in Fig. 3.13. Calcium cations that are bound only to PC in the mixed bilayer with PS behave similarly as in the pure PC bilayer maintaining comparable probabilities for clustering one, two, or even three PC lipids together. In contrast, PS lipids prefer 1:1 ratio with Ca^{2+}, which may also be due to their low molar fraction in the the mixed bilayer. In total, however, the negatively charged membrane has its stoichiometry shifted towards complexes with three phospholipids and one calcium. This is obviously due to the presence of POPS, which also contributes to the pre-formed one- and two-membered clusters of POPC. Clusters of four or more lipids were not observed in either membrane.

Timescales associated with the binding of calcium cations from solution to the membrane are plotted for each binding event as a histogram in Fig. 3.14. Using

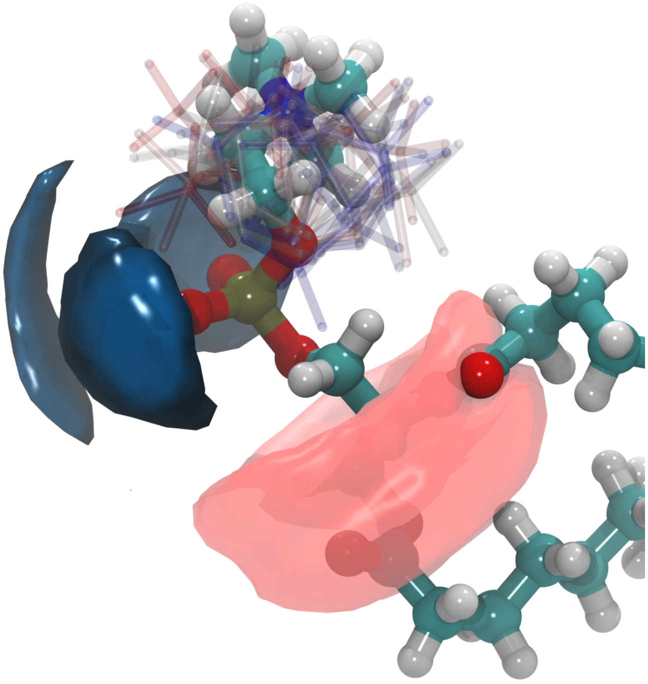

Figure 3.12: Isocontours of spatial number density of Ca^{2+} (dark blue, 0.001 $Å^{-3}$) and POPC carbonyl oxygen atoms (light semi-transparent red, 0.008 $Å^{-3}$, all POPC lipids contribute). Calcium cations localize mostly around phosphate oxygens (oxygens red, phosphorus bronze). Interactions with carbonyl oxygens is less likely than with phosphate oxygens, and it is contributed more by other neighbouring phospholipids than by the same lipid. Transparent structures are shown to depict the variability of choline configurations (colour warps from red to blue along the simulation time). The number density was evaluated for each lipid, after its structural alignment using only phosphate group. MDAnalysis [Michaud-Agrawal et al., 2011] library was used for the calculations of the structural alignment and the spatial number density. VMD [Humphrey et al., 1996] was used for visualization. Carbon atoms are depicted in cyan, hydrogen atoms in white, oxygen atoms in red, nitrogen in blue.

these plots, we can estimate that 90% of the residence times of any calcium cation will be lower than 60 ns for pure POPC neutral bilayer and shorter than 200 ns for the mixed 5 PC:1 PS negatively charged bilayer. The longest observed residence times in the simulations were 141 ns for the neutral membrane and 485 ns for the negatively charged membrane. Both estimates of the residence times come from simulations with comparable concentrations of around 250mM; the simulation with the neutral membrane has a bulk concentration of calcium C_{ion} = 280mM, whereas the simulation with the negatively charged membrane has a bulk concentration of calcium C_{ion} = 240mM.

In summary, the results from ECC-lipids suggest that the exchange of calcium between the POPC bilayer and the solvent occurs at the order of ∼10–100 ns, which is significantly faster than observed in simulations with other presently available non-polarizable models of lipids and ions [Javanainen et al., 2017, Catte et al., 2016]. Our results suggest that simulation trajectories with a characteristic length of several hundreds of nanoseconds are necessary to capture the binding of

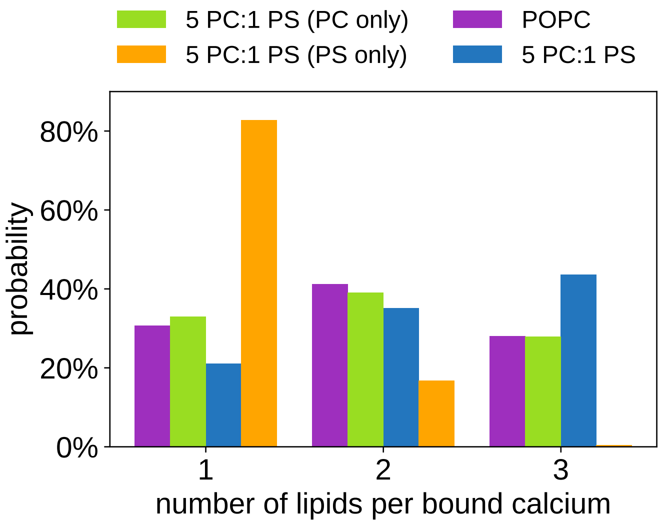

Figure 3.13: Relative probabilities of existence of Ca^{2+} complexes with a certain number of lipids. All lipids were taken into account with the exception of the complexes in light green and orange, for which we counted only contacts with POPC resp POPS from the mixed 5 PC:1 PS negatively charged bilayer. The calculated probabilities of the calcium-lipid complexes also reflect only POPC (light green) resp POPS (orange). Probabilities were taken from simulations with comparable bulk concentrations of calcium around 250 mM. Clusters of four or more lipids were not observed in either membrane.

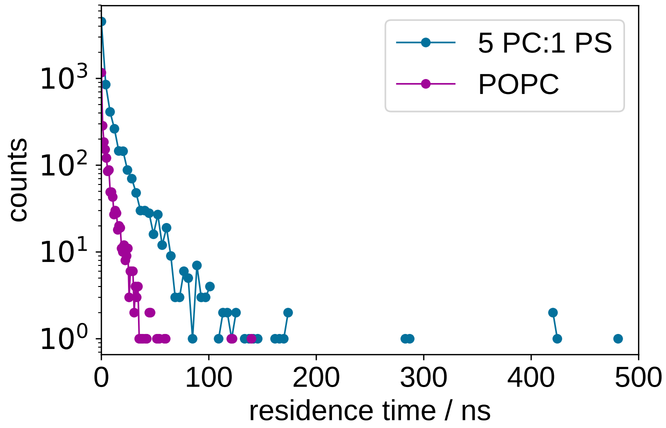

Figure 3.14: Histograms of residence times of Ca^{2+} in a neutral membrane composed of POPC (orange) and in a negatively charged membrane with the composition 5 PC:1 PS (blue) from simulations with ECC-lipids and ECC-ions. The simulation with the neutral membrane has a bulk concentration of calcium $C_{ion} = 280\text{mM}$, the simulation with the negatively charged membrane has a bulk concentration of calcium $C_{ion} = 240\text{mM}$. In the simulation with the neutral membrane, 90% of the residence times of calcium cations are shorter than 60 ns, with the longest observed residence time being 141 ns. In the simulation with the negatively charged membrane, 90% of the residence times of calcium cations are shorter than 200 ns, with the longest observed residence time being 485 ns.

calcium to neutral POPC bilayers in equilibrium when more realistic *polarizable* force fields are used. Interestingly enough, almost an order of magnitude longer simulations are required for the negatively charged bilayers.

Conclusion

Motivated by cellular processes, which involve ions and cell membranes as major actors, we have investigated model phospholipid membranes and their interactions with biologically relevant ions. The controlled concentrations of Na^+ and K^+ cations on either side of the membrane of neurons forms the transmembrane potential. Neurons vary the concentrations of theses cations to modulate the transmembrane potential and to conduct electrical signals along the axons. [Sten-Knudsen, 2002, Storace et al., 2015, Sung et al., 2015] In our work [Melcr et al., 2016], we compared two methods for modeling of the transmembrane potential in molecular simulations, i.e., the constant electric field method Roux [1997, 2008], Gumbart et al. [2012], and the ion imbalance method Sachs et al. [2004a], Kutzner et al. [2011]. We have proven the two methodologies to be equivalent, at least for electrolytes formed by the same monovalent ions on both sides of the membrane. While the structure of the bilayer remains almost unchanged by the transmembrane potential, the induced electric field in the hydrophobic core of the bilayer affects the orientation of water molecules at its interface highlighting its importance in electroporation. [Bu et al., 2017]

Next, we performed extensive sets of simulations of phospholipid bilayers with different salts at varying concentrations to study the binding of cations to model membranes. We used the most abundant representants of phospholipids to form neutral (POPC) or negatively charged (5 POPC:1 POPS) bilayers, for which we have provided a detailed insight into the interactions with Na^+, K^+, and Ca^{2+} cations. The affinity of the cations was measured using the concept of a lipid electrometer introduced by Seelig et al. [1987] and described in section 1.2. The head group order parameters α and β in POPC are experimentally observed to change proportionally to the bound charge per lipid. Such changes can then be related to the amount of bound ions.

In our publications [Catte et al., 2016, Bacle et al., 2018], we have shown that such order parameters can be accurately determined also from MD simulations and their changes correlate with the amount of bound charge in phospholipid bilayers, despite the inaccuracies in their actual structures without salts [Botan et al., 2015]. It was found, however, that none of the force fields examined in those works provided a sufficient accuracy for interpreting the experimentally measured structural changes induced by salt concentrations and cation-lipid stoichiometries. While there were several models that predicted realistic binding affinities of Na^+ to PC bilayers, all existing models overestimated the binding affinity of Ca^{2+} unless ad hoc specific repulsive potentials between the cations and the bilayer were applied. [Catte et al., 2016, Bacle et al., 2018] Thus, we identified the strong binding of Na^+ and Ca^{2+} cations in existing simulation models as a computational artifact. Such excessive amounts of cations would form effectively positively charged membranes even at physiological concentrations affecting interactions with any charged molecules. For instance, the total charge of proteins in prokaryotes and also eukaryotes is mostly negative, [Link et al., 1997a,b, Urquhart et al., 1998, Schwartz et al., 2001, Knight et al., 2004] Thus, positively charged membranes would promote non-specific adsorption of proteins on their surface contrary to experiment. [Junková et al., 2016, Lingwood and

Simons, 2010, Sekereš et al., 2015]

A major improvement over currently available non-polarizable force fields was achieved by developing new models of phospholipids, the so called ECC-lipids, which are described in section 2.3 and in the publication [Melcr et al., 2018]. In contrast to the models studied in the works [Catte et al., 2016, Bacle et al., 2018], ECC-lipids account for electronic polarization via the electronic continuum correction, which was introduced in section 2.2. In short, ECC is an implicit model of electronic polarizability, which can be straightforwardly implemented into current force fields by scaling charges. In section 2.3, we demonstrated on the cases of PC, PS, and PE phospholipids that it is sufficient to also scale the Lennard-Jones parameters σ of the affected atoms to reach a structural agreement with x-ray scattering experiments. Our new model, ECC-lipids, provides a proof of concept of the applicability of ECC to charged as well as neutral molecules.

Our simulations with ECC-lipids suggest that Na^+ and Ca^{2+} cations interact specifically with the phosphate and carboxylate groups of PC and PS and occasionally also with the carbonyl groups. K^+ interacts only very weakly with the bilayers affecting slightly only carboxylate groups in POPS, which are more exposed to the solvent compared to phosphate groups. In overall, weaker binding of cations to phospholipid bilayers is observed compared to previous MD simulation studies [Bacle et al., 2018, Catte et al., 2016, Böckmann et al., 2003, Böckmann and Grubmüller, 2004, Melcrová et al., 2016, Javanainen et al., 2017]. Importantly, our simulations show for the first time a *quantitative* agreement with the experimental lipid electrometer concept for POPC and also for POPS with all the studied cations. For instance, the small differences in the responses of the order parameter β in POPS between the Na^+, K^+, and Ca^{2+} cations are captured well by our model. Also, the exchange of calcium between a phospholipid bilayer and solvent occurs at the order of 10–100 ns, which is in accord with experiments and also significantly faster than the time scales from simulations with other presently available non-polarizable models of lipids [Melcrová et al., 2016, Javanainen et al., 2017, Catte et al., 2016]. Nevertheless, even with ECC-lipids, the reversible process of calcium binding to phospholipid bilayers in equilibrium requires simulations of a characteristic length of several hundreds of nanoseconds for the neutral bilayers, while almost an order of magnitude longer lengths are required for the negatively charged bilayers. In summary, our results are in accordance with the works, which suggest that monovalent cations (with the exception of Li^+) exhibit negligible binding to phospholipid bilayers, while multivalent cations interact significantly [Cevc, 1990, Tocanne and Teissié, 1990, Hauser et al., 1976, 1978, Herbette et al., 1984, Altenbach and Seelig, 1984, Clarke and Lüpfert, 1999, Binder and Zschörnig, 2002, Pabst et al., 2007, Uhríková et al., 2008, Filippov et al., 2009].

Treatment of the electronic polarization was shown to have a dramatically positive impact on the accuracy of the description of interactions between phospholipids and cations. The presented application of ECC to lipids constitutes a pivotal work for its future adaptations to also other compounds, especially charged and zwitterionic, e.g., proteins or nucleic acids, for which we expect improvements in computational description in a similar range.

Bibliography

Hideo Akutsu and Joachim Seelig. Interaction of metal ions with phosphatidylcholine bilayer membranes. *Biochemistry*, 20:7366–7373, 1981.

B Alberts, A Johnson, J Lewis, M Raff, K Roberts, and P And Walter. *Molecular Biology of the Cell*. Garland Press: New York, 2008. ISBN 0815341067.

Christian Altenbach and Joachim Seelig. Calcium binding to phosphatidylcholine bilayers as studied by deuterium magnetic resonance. evidence for the formation of a calcium complex with two phospholipid molecules. *Biochemistry*, 23:3913–3920, 1984.

Ida Annunziata and Alessandra D'Azzo. Interorganellar Membrane Microdomains: Dynamic Platforms in the Control of Calcium Signaling and Apoptosis. *Cells*, 2(3):574–590, aug 2013. ISSN 2073-4409. doi: 10.3390/cells2030574. URL `http://www.mdpi.com/2073-4409/2/3/574`.

Amelie Bacle, Pavel Buslaev, Lukasz Cwiklik, Fernando Favela, Tiago Ferreira, Patrick Fuchs, Ivan Gushchin, Matti Javanainen, Batuhan Kav, Jesper Madsen, Josef Melcr, Markus Miettinen, Ricky Nencini, Samuli Ollila, Chris Papadopoulos, and Thomas Piggot. Head group and glycerol backbone structures, and cation binding in bilayers with PS lipids. 2018.

Ci Christopher I Bayly, Piotr Cieplak, Wendy D Cornell, and Peter A Kollman. A well-behaved electrostatic potential based method using charge restraints for deriving atomic charges: the RESP model. *J. Phys. Chem.*, 97:10269–10280, 1993. ISSN 0022-3654. doi: 10.1021/j100142a004. URL `http://pubs.acs.org/doi/abs/10.1021/j100142a004`.

Witali Beichel, Nils Trapp, Christoph Hauf, Oliver Kohler, Georg Eickerling, Wolfgang Scherer, and Ingo Krossing. Charge-scaling effect in ionic liquids from the charge-density analysis of n,n′-dimethylimidazolium methylsulfate. *Ang. Chem. Int. Ed.*, 53(12):3143–3146, 2014. ISSN 1521-3773. doi: 10.1002/anie.201308760. URL `http://dx.doi.org/10.1002/anie.201308760`.

A. L. Benavides, M. A. Portillo, V. C. Chamorro, J. R. Espinosa, J. L. F. Abascal, and C. Vega. A potential model for sodium chloride solutions based on the tip4p/2005 water model. *J. Chem. Phys.*, 147(10):104501, 2017.

O. Berger, O. Edholm, and F. Jähnig. Molecular dynamics simulations of a fluid bilayer of dipalmitoylphosphatidylcholine at full hydration, constant pressure, and constant temperature. *Biophys. J.*, 72:2002 – 2013, 1997.

Max L. Berkowitz and Robert Vacha. Aqueous solutions at the interface with phospholipid bilayers. *Acc. Chem. Res.*, 45:74–82, 2012.

Max L. Berkowitz, David L. Bostick, and Sagar Pandit. Aqueous solutions next to phospholipid membrane surfaces: Insights from simulations. *Chem. Rev.*, 106:1527–1539, 2006.

Michael J. Berridge, Martin D. Bootman, and H. Llewelyn Roderick. Calcium signalling: dynamics, homeostasis and remodelling. *Nature Reviews Molecular Cell Biology*, 4(7):517–529, jul 2003. ISSN 1471-0072. doi: 10.1038/nrm1155. URL `http://www.nature.com/articles/nrm1155`.

Georgi Beschiaschvili and Joachim Seelig. Peptide binding to lipid membranes. spectroscopic studies on the insertion of a cyclic somatostatin analog into phospholipid bilayers. *Biochim. Biophys. Acta*, 1061(1):78 – 84, 1991.

Francisco Bezanilla. Ion channels: from conductance to structure. *Neuron*, 60(3): 456–68, nov 2008. ISSN 1097-4199. doi: 10.1016/j.neuron.2008.10.035. URL `http://www.cell.com/article/S0896627308009008/fulltext`.

Eva Bilkova, Roman Pleskot, Sami Rissanen, Simou Sun, Aleksander Czogalla, Lukasz Cwiklik, Tomasz Róg, Ilpo Vattulainen, Paul S Cremer, Pavel Jungwirth, and Ünal Coskun. Calcium directly regulates phosphatidylinositol 4,5-bisphosphate headgroup conformation and recognition. *J. Am. Chem. Soc.*, 139:4019–4024, 2017. doi: 10.1021/jacs.6b11760.

Hans Binder and Olaf Zschörnig. The effect of metal cations on the phase behavior and hydration characteristics of phospholipid membranes. *Chem. Phys. Lipids*, 115:39 – 61, 2002.

Rainer A. Böckmann and Helmut Grubmüller. Multistep binding of divalent cations to phospholipid bilayers: A molecular dynamics study. *Ang. Chem. Int. Ed.*, 43:1021–1024, 2004.

Rainer A. Böckmann, Agnieszka Hac, Thomas Heimburg, and Helmut Grubmüller. Effect of sodium chloride on a lipid bilayer. *Biophys. J.*, 85:1647 – 1655, 2003.

Rainer A. Böckmann, Bert L. de Groot, Sergej Kakorin, Eberhard Neumann, and Helmut Grubmüller. Kinetics, Statistics, and Energetics of Lipid Membrane Electroporation Studied by Molecular Dynamics Simulations. *Biophys. J.*, 95(4):1837–1850, August 2008. ISSN 0006-3495. doi: 10.1529/biophysj.108.129437. URL `http://www.sciencedirect.com/science/article/pii/S0006349508701449`.

Alexandru Botan, Fernando Favela-Rosales, Patrick F. J. Fuchs, Matti Javanainen, Matej Kanduč, Waldemar Kulig, Antti Lamberg, Claire Loison, Alexander Lyubartsev, Markus S. Miettinen, Luca Monticelli, Jukka Määttä, O. H. Samuli Ollila, Marius Retegan, Tomasz Róg, Hubert Santuz, and Joona Tynkkynen. Toward atomistic resolution structure of phosphatidylcholine headgroup and glycerol backbone at different ambient conditions. *J. Phys. Chem. B*, 119(49):15075–15088, 2015.

M. F. Brown and J. Seelig. Ion-induced changes in head group conformation of lecithin bilayers. *Nature*, 269:721–723, 1977.

Jeffrey L. Browning and Joachim Seelig. Bilayers of phosphatidylserine: a deuterium and phosphorus nuclear magnetic resonance study. *Biochemistry*, 19(6): 1262–1270, 1980.

Bing Bu, Dechang Li, Jiajie Diao, and Baohua Ji. Mechanics of water pore formation in lipid membrane under electric field. *Acta Mechanica Sinica*, 33 (2):234–242, 2017.

M. Casciola, D. Bonhenry, M. Liberti, F. Apollonio, and M. Tarek. A molecular dynamic study of cholesterol rich lipid membranes: comparison of electroporation protocols. *Bioelectrochemistry*, 100:11–17, December 2014. ISSN 1567-5394. doi: 10.1016/j.bioelechem.2014.03.009. URL `http://www.sciencedirect.com/science/article/pii/S1567539414000619`.

Andrea Catte, Mykhailo Girych, Matti Javanainen, Claire Loison, Josef Melcr, Markus S. Miettinen, Luca Monticelli, Jukka Maatta, Vasily S. Oganesyan, O. H. Samuli Ollila, Joona Tynkkynen, and Sergey Vilov. Molecular electrometer and binding of cations to phospholipid bilayers. *Phys. Chem. Chem. Phys.*, 18:32560–32569, 2016.

David S. Cerutti, Julia E. Rice, William C. Swope, and David A. Case. Derivation of fixed partial charges for amino acids accommodating a specific water model and implicit polarization. *J. Phys. Chem. B*, 117(8):2328–2338, 2013. doi: 10.1021/jp311851r. URL `http://dx.doi.org/10.1021/jp311851r`.

Gregor Cevc. Membrane electrostatics. *Biochim. Biophys. Acta*, 1031:311 – 382, 1990.

D. K. Chattoraj and K. S. Birdi. *Adsorption at the Liquid Interface from the Multicomponent Solution*, pages 83–131. Springer US, Boston, MA, 1984. ISBN 978-1-4615-8333-2. doi: 10.1007/978-1-4615-8333-2_4. URL `https://doi.org/10.1007/978-1-4615-8333-2_4`.

Wah Chiu and Kenneth H Downing. Editorial overview: Cryo electron microscopy: Exciting advances in cryoem herald a new era in structural biology. *Current opinion in structural biology*, 46:iv, 2017.

A. K. Chouhan, M. V. Ivannikov, Z. Lu, M. Sugimori, R. R. Llinas, and G. T. Macleod. Cytosolic Calcium Coordinates Mitochondrial Energy Metabolism with Presynaptic Activity. *Journal of Neuroscience*, 32(4):1233–1243, jan 2012. ISSN 0270-6474. doi: 10.1523/JNEUROSCI.1301-11.2012. URL `http://www.jneurosci.org/cgi/doi/10.1523/JNEUROSCI.1301-11.2012`.

Janamejaya Chowdhary, Edward Harder, Pedro E. M. Lopes, Lei Huang, Alexander D. MacKerell, and Benoît Roux. A polarizable force field of dipalmitoylphosphatidylcholine based on the classical drude model for molecular dynamics simulations of lipids. *J. Phys. Chem. B*, 117(31):9142–9160, 2013.

David E. Clapham. Calcium Signaling. *Cell*, 131(6):1047–1058, dec 2007. ISSN 00928674. doi: 10.1016/j.cell.2007.11.028. URL `http://linkinghub.elsevier.com/retrieve/pii/S0092867407015310`.

Ronald J. Clarke and Christian Lüpfert. Influence of Anions and Cations on the Dipole Potential of Phosphatidylcholine Vesicles: A Basis for the Hofmeister Effect. *Biophys. J.*, 76(5):2614 – 2624, 1999.

Arnau Cordomí, Olle Edholm, and Juan J. Perez. Effect of ions on a dipalmitoyl phosphatidylcholine bilayer. a molecular dynamics simulation study. *J. Phys. Chem. B*, 112(5):1397–1408, 2008.

Arnau Cordomí, Olle Edholm, and Juan J. Perez. Effect of force field parameters on sodium and potassium ion binding to dipalmitoyl phosphatidylcholine bilayers. *J. Chem. Theory Comput.*, 5:2125–2134, 2009.

Tom Darden, Darrin York, and Lee Pedersen. Particle mesh ewald: An n·log(n) method for ewald sums in large systems. *J. Chem. Phys.*, 98(12):10089–10092, 1993.

James H. Davis. The description of membrane lipid conformation, order and dynamics by 2h-nmr. *Biochim. Biophys. Acta*, 737(1):117 – 171, 1983.

Lucie Delemotte, François Dehez, Werner Treptow, and Mounir Tarek. Modeling membranes under a transmembrane potential. *J. Phys. Chem. B*, 112(18): 5547–50, May 2008. ISSN 1520-6106. doi: 10.1021/jp710846y. URL `http://www.ncbi.nlm.nih.gov/pubmed/18412411`.

Callum J. Dickson, Benjamin D. Madej, Åge A. Skjevik, Robin M. Betz, Knut Teigen, Ian R. Gould, and Ross C. Walker. Lipid14: The Amber Lipid Force Field. *J. Chem. Theory Comput.*, 10(2):865–879, 2014.

Egbert Egberts, Siewert-Jan Marrink, and Herman J. C. Berendsen. Molecular dynamics simulation of a phospholipid membrane. *Eur. Biophys. J.*, 22(6): 423–436, 1994.

Moises Eisenberg, Thomas Gresalfi, Thomas Riccio, and Stuart McLaughlin. Adsorption of monovalent cations to bilayer membranes containing negative phospholipids. *Biochemistry*, 18(23):5213–5223, 1979.

U. L. Essman, M. L. Perera, M. L. Berkowitz, T. Larden, H. Lee, and L. G. Pedersen. A smooth particle mesh ewald potential. *J. Chem. Phys.*, 103:8577–8592, 1995.

UrsM. Ferber, Gillian Kaggwa, and SuzanneP. Jarvis. Direct imaging of salt effects on lipid bilayer ordering at sub-molecular resolution. *Eur. Biophys. J.*, 40(3):329–338, 2011. ISSN 0175-7571. doi: 10.1007/s00249-010-0650-7. URL `http://dx.doi.org/10.1007/s00249-010-0650-7`.

Tiago Mendes Ferreira, Filipe Coreta-Gomes, O. H. Samuli Ollila, Maria Joao Moreno, Winchil L. C. Vaz, and Daniel Topgaard. Cholesterol and POPC segmental order parameters in lipid membranes: solid state ^{1}H-^{1}3C NMR and MD simulation studies. *Phys. Chem. Chem. Phys.*, 15:1976–1989, 2013.

Tiago Mendes Ferreira, Rohit Sood, Ruth Bärenwald, Göran Carlström, Daniel Topgaard, Kay Saalwächter, Paavo K. J. Kinnunen, and O. H. Samuli Ollila. Acyl chain disorder and azelaoyl orientation in lipid membranes containing oxidized lipids. *Langmuir*, 32(25):6524–6533, 2016.

Andrey Filippov, Greger Orädd, and Göran Lindblom. Effect of NaCl and $CaCl_2$ on the lateral diffusion of zwitterionic and anionic lipids in bilayers. *Chem. Phys. Lipids*, 159(2):81 – 87, 2009.

Lea Fink, Jehuda Feitelson, Roy Noff, Tom Dvir, Carmen Tamburu, and Uri Raviv. Osmotic stress induced desorption of calcium ions from dipolar lipid membranes. *Langmuir*, 33(23):5636–5641, 2017.

Ran Friedman, Syma Khalid, Camilo Aponte-Santamaría, Elena Arutyunova, Marlon Becker, Kevin J. Boyd, Mikkel Christensen, João T. S. Coimbra, Simona Concilio, Csaba Daday, Floris J. van Eerden, Pedro A. Fernandes, Frauke Gräter, Davit Hakobyan, Andreas Heuer, Konstantina Karathanou, Fabian Keller, M. Joanne Lemieux, Siewert J. Marrink, Eric R. May, Antara Mazumdar, Richard Naftalin, Mónica Pickholz, Stefano Piotto, Peter Pohl, Peter Quinn, Maria J. Ramos, Birgit Schiøtt, Durba Sengupta, Lucia Sessa, Stefano Vanni, Talia Zeppelin, Valeria Zoni, Ana-Nicoleta Bondar, and Carmen Domene. Understanding conformational dynamics of complex lipid mixtures relevant to biology. *Journal of Membrane Biology (submitted)*, 2018.

Takeshi Fukuma, Michael J. Higgins, and Suzanne P. Jarvis. Direct imaging of lipid-ion network formation under physiological conditions by frequency modulation atomic force microscopy. *Phys. Rev. Lett.*, 98:106101, 2007.

Hans Ulrich Gally, Gerd Pluschke, Peter Overath, and Joachim Seelig. Structure of escherichia coli membranes. glycerol auxotrophs as a tool for the analysis of the phospholipid head-group region by deuterium magnetic resonance. *Biochemistry*, 20(7):1826–1831, 1981.

Juan J. Garcia-Celma, Lina Hatahet, Werner Kunz, and Klaus Fendler. Specific anion and cation binding to lipid membranes investigated on a solid supported membrane. *Langmuir*, 23(20):10074–10080, 2007.

Sergi Garcia-Manyes, Gerard Oncins, and Fausto Sanz. Effect of ion-binding and chemical phospholipid structure on the nanomechanics of lipid bilayers studied by force spectroscopy. *Biophys. J.*, 89:1812 – 1826, 2005.

Sergi Garcia-Manyes, Gerard Oncins, and Fausto Sanz. Effect of pH and ionic strength on phospholipid nanomechanics and on deposition process onto hydrophilic surfaces measured by AFM . *Electrochim. Acta*, 51(24):5029 – 5036, 2006. ISSN 0013-4686. doi: http://dx.doi.org/10.1016/j.electacta.2006.03.062.

Mykhailo Girych and O. H. Samuli Ollila. Popc_amber_lipid14_verlet, September 2015a. URL `http://dx.doi.org/10.5281/zenodo.30898`.

Mykhailo Girych and O. H. Samuli Ollila. Popc_amber_lipid14_nacl_1mol, September 2015b. URL `http://dx.doi.org/10.5281/zenodo.30865`.

Mykhailo Girych and O. H. Samuli Ollila. Popc_amber_lipid14_cacl2_035mol, November 2015c. URL `http://dx.doi.org/10.5281/zenodo.34415`.

Mykhailo Girych and Samuli Ollila. Popc_amber_lipid14_cacl2_035mol, February 2016. URL `https://doi.org/10.5281/zenodo.46234`.

Brian Glancy, Wayne T. Willis, David J. Chess, and Robert S. Balaban. Effect of Calcium on the Oxidative Phosphorylation Cascade in Skeletal Muscle Mitochondria. *Biochemistry*, 52(16):2793–2809, apr 2013. ISSN 0006-2960. doi: 10.1021/bi3015983. URL `http://pubs.acs.org/doi/10.1021/bi3015983`.

I.R. Gould, A.A. Skjevik, C.J. Dickson, B.D. Madej, and R.C. Walker. Lipid17: A comprehensive amber force field for the simulation of zwitterionic and anionic lipids, 2018. In preparation.

James Gumbart, Fatemeh Khalili-Araghi, Marcos Sotomayor, and Benoît Roux. Constant electric field simulations of the membrane potential illustrated with simple systems. *Biochim. Biophys. Acta, Biomembr.*, 1818(2):294–302, February 2012. ISSN 0005-2736. doi: 10.1016/j.bbamem.2011.09.030. URL `http://www.sciencedirect.com/science/article/pii/S0005273611003361`.

Frédéric F. Harb and Bernard Tinland. Effect of ionic strength on dynamics of supported phosphatidylcholine lipid bilayer revealed by frapp and langmuir–blodgett transfer ratios. *Langmuir*, 29(18):5540–5546, 2013.

H. Hauser, M. C. Phillips, B. Levine, and R.J.P. Williams. Conformation of the lecithin polar group in charged vesicles. *Nature*, 261:390 – 394, 1976.

H. Hauser, W. Guyer, B. Levine, P. Skrabal, and R.J.P. Williams. The conformation of the polar group of lysophosphatidylcholine in h2o; conformational changes induced by polyvalent cations. *Biochim. Biophys. Acta*, 508(3):450 – 463, 1978. ISSN 0005-2736. doi: http://dx.doi.org/10.1016/0005-2736(78)90091-3. URL `http://www.sciencedirect.com/science/article/pii/0005273678900913`.

L. Herbette, C.A. Napolitano, and R.V. McDaniel. Direct determination of the calcium profile structure for dipalmitoyllecithin multilayers using neutron diffraction. *Biophys. J.*, 46(6):677 – 685, 1984.

Hao Hu, Zhenyu Lu, and and Weitao Yang. Fitting Molecular Electrostatic Potentials from Quantum Mechanical Calculations. *J. Chem. Theory Comput.*, 3(3):1004–1013, 2007. ISSN 1549-9618. doi: 10.1021/ct600295n. URL `http://dx.doi.org/10.1021/ct600295n`.

Jing Huang, Andrew C Simmonett, Frank C Pickard IV, Alexander D MacKerell Jr, and Bernard R Brooks. Mapping the drude polarizable force field onto a multipole and induced dipole model. *The Journal of chemical physics*, 147 (16):161702, 2017.

William Humphrey, Andrew Dalke, and Klaus Schulten. VMD – Visual Molecular Dynamics. *J. Mol. Graphics*, 14:33–38, 1996.

Joakim P. M. Jämbeck and Alexander P. Lyubartsev. Derivation and systematic validation of a refined all-atom force field for phosphatidylcholine lipids. *J. Phys. Chem. B*, 116(10):3164–3179, 2012a.

Joakim P. M. Jämbeck and Alexander P. Lyubartsev. An extension and further validation of an all-atomistic force field for biological membranes. *J. Chem. Theory Comput.*, 8(8):2938–2948, 2012b.

Matti Javanainen, Adéla Melcrová, Aniket Magarkar, Piotr Jurkiewicz, Martin Hof, Pavel Jungwirth, and Hector Martinez-Seara. Two cations, two mechanisms: interactions of sodium and calcium with zwitterionic lipid membranes. *Chem. Commun.*, 53:5380–5383, 2017. doi: 10.1039/C7CC02208E. URL `http://dx.doi.org/10.1039/C7CC02208E`.

Sunhwan Jo, Taehoon Kim, Vidyashankara G. Iyer, and Wonpil Im. CHARMM-GUI: A web-based graphical user interface for CHARMM. *J. Comput. Chem.*, 29(11):1859–1865, 2008.

E. Jones, T. Oliphant, P. Peterson, and et. al. SciPy: Open source scientific tools for Python, 2001–2018. URL `http://www.scipy.org/`. [Online; accessed Dec-2017].

B. Jönsson, O. Edholm, and O. Teleman. Molecular dynamics simulations of a sodium octanoate micelle in aqueous solution. *J. Chem. Phys.*, 85:2259–2271, 1986.

William L. Jorgensen, David S. Maxwell, and Julian Tirado-Rives. Development and Testing of the OPLS All-Atom Force Field on Conformational Energetics and Properties of Organic Liquids. *J. Am. Chem. Soc.*, 118(45):11225–11236, 1996.

P Junková, J Prchal, V Spiwok, R Pleskot, J Kadlec, L Krásný, R Hynek, R Hrabal, and T Ruml. Molecular aspects of the interaction between Mason—Pfizer monkey virus matrix protein and artificial phospholipid membrane. *Proteins: Structure, Function, and Bioinformatics*, 84(11):1717–1727, 2016.

Benjamin Klasczyk, Volker Knecht, Reinhard Lipowsky, and Rumiana Dimova. Interactions of alkali metal chlorides with phosphatidylcholine vesicles. *Langmuir*, 26(24):18951–18958, 2010.

Jeffery B. Klauda, Richard M. Venable, J. Alfredo Freites, Joseph W. O'Connor, Douglas J. Tobias, Carlos Mondragon-Ramirez, Igor Vorobyov, Alexander D. MacKerell Jr, and Richard W. Pastor. Update of the CHARMM all-atom additive force field for lipids: Validation on six lipid types. *J. Phys. Chem. B*, 114:7830–7843, 2010.

Christopher G Knight, Rees Kassen, Holger Hebestreit, and Paul B Rainey. Global analysis of predicted proteomes: functional adaptation of physical properties. *Proceedings of the National Academy of Sciences*, 101(22):8390–8395, 2004.

Miriam Kohagen, Philip E. Mason, and Pavel Jungwirth. Accurate description of calcium solvation in concentrated aqueous solutions. *J. Phys. Chem. B*, 118 (28):7902–7909, 2014.

Miriam Kohagen, Philip E. Mason, and Pavel Jungwirth. Accounting for electronic polarization effects in aqueous sodium chloride via molecular dynamics aided by neutron scattering. *J. Phys. Chem. B*, 120(8):1454–1460, 2016.

N. Kučerka, M. P. Nieh, and J. Katsaras. Fluid phase lipid areas and bilayer thicknesses of commonly used phosphatidylcholines as a function of temperature. *Biochim. Biophys. Acta*, 1808(11):2761–2771, 2011. ISSN 0006-3002.

Waldemar Kulig, Joona Tynkkynen, Matti Javanainen, Moutusi Manna, Tomasz Rog, Ilpo Vattulainen, and Pavel Jungwirth. How well does cholesteryl hemisuccinate mimic cholesterol in saturated phospholipid bilayers? *Journal of Molecular Modeling*, 20(2):2121, 2014. ISSN 1610-2940.

Waldemar Kulig, Piotr Jurkiewicz, Agnieszka Olżyńska, Joona Tynkkynen, Matti Javanainen, Moutusi Manna, Tomasz Rog, Martin Hof, Ilpo Vattulainen, and Pavel Jungwirth. Experimental determination and computational interpretation of biophysical properties of lipid bilayers enriched by cholesteryl hemisuccinate. *Biochim. Biophys. Acta*, 1848(2):422 – 432, 2015.

Carsten Kutzner, Helmut Grubmüller, Bert L. de Groot, and Ulrich Zachariae. Computational Electrophysiology: The Molecular Dynamics of Ion Channel Permeation and Selectivity in Atomistic Detail. *Biophys. J.*, 101(4):809–817, August 2011. ISSN 0006-3495. doi: 10.1016/j.bpj.2011.06.010. URL `http://www.sciencedirect.com/science/article/pii/S0006349511007065`.

Jumin Lee, Xi Cheng, Jason M. Swails, Min Sun Yeom, Peter K. Eastman, Justin A. Lemkul, Shuai Wei, Joshua Buckner, Jong Cheol Jeong, Yifei Qi, Sunhwan Jo, Vijay S. Pande, David A. Case, III Charles L. Brooks, Jr. Alexander D. MacKerell, Jeffery B. Klauda, and Wonpil Im. CHARMM-GUI Input Generator for NAMD, GROMACS, AMBER, OpenMM, and CHARMM/OpenMM Simulations Using the CHARMM36 Additive Force Field. *J. Chem. Theory Comput.*, 12(1):405–413, 2016.

Sarah Lee, Alan Tran, Matthew Allsopp, Joseph B. Lim, Jérôme Henin, and Jeffery B. Klauda. Charmm36 united atom chain model for lipids and surfactants. *J. Phys. Chem. B*, 118(2):547–556, 2014.

Justin A Lemkul, Jing Huang, Benoît Roux, and Alexander D MacKerell Jr. An empirical polarizable force field based on the classical drude oscillator model: development history and recent applications. *Chemical reviews*, 116(9):4983–5013, 2016.

E. Leontidis and A. Aroti. Liquid expanded monolayers of lipids as model systems to understand the anionic hofmeister series: 2. ion partitioning is mostly a matter of size. *J. Phys. Chem. B*, 113(5):1460–1467, 2009.

I. V. Leontyev and A. A. Stuchebrukhov. Electronic continuum model for molecular dynamics simulations. *J. Chem. Phys.*, 130(8):085102, feb 2009. ISSN 1089-7690. doi: 10.1063/1.3060164. URL `http://scitation.aip.org/content/aip/journal/jcp/130/8/10.1063/1.3060164`.

I. V. Leontyev and A. A. Stuchebrukhov. Electronic Continuum Model for Molecular Dynamics Simulations of Biological Molecules. *J. Chem. Theory Comput.*, 6(5):1498–1508, may 2010. ISSN 1549-9618. doi: 10.1021/ct9005807. URL `http://dx.doi.org/10.1021/ct9005807`.

Igor Leontyev and Alexei Stuchebrukhov. Accounting for electronic polarization in non-polarizable force fields. *Phys. Chem. Chem. Phys.*, 13:2613–2626, 2011.

Igor V. Leontyev and Alexei A. Stuchebrukhov. Polarizable molecular interactions in condensed phase and their equivalent nonpolarizable models. *J. Chem. Phys.*, 141(1):014103, jul 2014. ISSN 00219606. doi: 10.1063/1.4884276. URL `http://aip.scitation.org/doi/10.1063/1.4884276`.

Daniel Lingwood and Kai Simons. Lipid rafts as a membrane-organizing principle. *Science*, 327(5961):46–50, 2010.

Andrew J Link, Lara G Hays, Edwin B Carmack, and John R Yates III. Identifying the major proteome components of haemophilus influenzae type-strain nctc 8143. *Electrophoresis*, 18(8):1314–1334, 1997a.

Andrew J Link, Keith Robison, and George M Church. Comparing the predicted and observed properties of proteins encoded in the genome of escherichia coli k-12. *Electrophoresis*, 18(8):1259–1313, 1997b.

Timothy R. Lucas, Brad A. Bauer, and Sandeep Patel. Charge equilibration force fields for molecular dynamics simulations of lipids, bilayers, and integral membrane protein systems. *Biochim. Biophys. Acta*, 1818(2):318 – 329, 2012.

Arkadiusz Maciejewski, Marta Pasenkiewicz-Gierula, Oana Cramariuc, Ilpo Vattulainen, and Tomasz Rog. Refined opls all-atom force field for saturated phosphatidylcholine bilayers at full hydration. *J. Phys. Chem. B*, 118(17): 4571–4581, 2014.

Aniket Magarkar, Piotr Jurkiewicz, Christoph Allolio, Martin Hof, and Pavel Jungwirth. Increased Binding of Calcium Ions at Positively Curved Phospholipid Membranes. *Journal of Physical Chemistry Letters*, 8(2):518–523, jan 2017. ISSN 19487185. doi: 10.1021/acs.jpclett.6b02818. URL `http://pubs.acs.org/doi/abs/10.1021/acs.jpclett.6b02818`.

S.J. Marrink, H.J. Risselada, S. Yefimov, D.P. Tieleman, and A.H. de Vries. The MARTINI forcefield: coarse grained model for biomolecular simulations. *J. Phys. Chem. B*, 111:7812–7824, 2007.

D. Marsh. *Handbook of Lipid Bilayers, Second Edition.* RSC press, 2013.

Tomáš Martínek, Elise Duboué-Dijon, Štěpán Timr, Philip E Mason, Katarina Baxová, Henry E Fischer, Burkhard Schmidt, Eva Pluhařová, and Pavel Jungwirth. Calcium ions in aqueous solutions: Accurate force field description aided by ab initio molecular dynamics and neutron scattering, 2018.

Josef Melcr, Daniel Bonhenry, Štěpán Timr, and Pavel Jungwirth. Transmembrane Potential Modeling: Comparison between Methods of Constant Electric Field and Ion Imbalance. *Journal of Chemical Theory and Computation*, 12 (5):2418–2425, apr 2016. ISSN 15499626. doi: 10.1021/acs.jctc.5b01202. URL `http://dx.doi.org/10.1021/acs.jctc.5b01202`.

Josef Melcr, Hector Martinez-Seara, Ricky Nencini, Jiří Kolafa, Pavel Jungwirth, and O. H. Samuli Ollila. Accurate binding of sodium and calcium to a popc bilayer by effective inclusion of electronic polarization. *The Journal of Physical Chemistry B*, 122(16):4546–4557, 2018. doi: 10.1021/acs.jpcb.7b12510. URL `https://doi.org/10.1021/acs.jpcb.7b12510`. PMID: 29608850.

Adéla Melcrová, Šárka Pokorná, Saranya Pullanchery, Miriam Kohagen, Piotr Jurkiewicz, Martin Hof, Pavel Jungwirth, Paul S. Cremer, and Lukasz Cwiklik. The complex nature of calcium cation interactions with phospholipid bilayers. *Sci. Reports*, 6:38035, 2016.

M. Michalak, Robert J.M. Parker, and M. Opas. Ca^{2+} signaling and calcium binding chaperones of the endoplasmic reticulum. *Cell Calcium*, 32(5-6):269–278, nov 2002. ISSN 01434160. doi: 10.1016/S0143416002001884. URL `http://linkinghub.elsevier.com/retrieve/pii/S0143416002001884`.

Naveen Michaud-Agrawal, Elizabeth J. Denning, Thomas B. Woolf, and Oliver Beckstein. Mdanalysis: A toolkit for the analysis of molecular dynamics simulations. *Journal of Computational Chemistry*, 32(10):2319–2327, 2011. ISSN 1096-987X. doi: 10.1002/jcc.21787. URL `http://dx.doi.org/10.1002/jcc.21787`.

Markus S. Miettinen and O. H. S. Ollila. The NMRlipids project – Open Collaboration to understand lipid systems in atomistic resolution, 2018. URL `http://nmrlipids.blogspot.fi/`.

Ole G Mouritsen. Model answers to lipid membrane questions. *Cold Spring Harb. Perspect. Biol.*, 3(9):a004622, September 2011. ISSN 1943-0264. doi: 10.1101/cshperspect.a004622. URL `http://cshperspectives.cshlp.org/content/3/9/a004622.full`.

Eva Nogales. The development of cryo-em into a mainstream structural biology technique. *Nature methods*, 13(1):24, 2015.

O.H. Samuli Ollila and Georg Pabst. Atomistic resolution structure and dynamics of lipid bilayers in simulations and experiments. *Biochim. Biophys. Acta*, 1858 (10):2512 – 2528, 2016.

Abraham Olusegun Oluwole, Bartholomäus Danielczak, Annette Meister, Jonathan Oyebamiji Babalola, Carolyn Vargas, and Sandro Keller. Solubilization of membrane proteins into functional lipid-bilayer nanodiscs using a diisobutylene/maleic acid copolymer. *Angewandte Chemie International Edition*, 56(7):1919–1924, 2017.

Georg Pabst, Aden Hodzic, Janez Strancar, Sabine Danner, Michael Rappolt, and Peter Laggner. Rigidification of neutral lipid bilayers in the presence of salts. *Biophys. J.*, 93:2688 – 2696, 2007.

Jianjun Pan, Xiaolin Cheng, Luca Monticelli, Frederick A Heberle, Norbert Kučerka, D Peter Tieleman, and John Katsaras. The molecular structure of a phosphatidylserine bilayer determined by scattering and molecular dynamics simulations. *Soft Matter*, 10(21):3716–3725, 2014.

Jean-Philip Piquemal, Lalith Perera, G Andrés Cisneros, Pengyu Ren, Lee G Pedersen, and Thomas A Darden. Towards accurate solvation dynamics of divalent cations in water using the polarizable amoeba force field: From energetics to structure. *The Journal of chemical physics*, 125(5):054511, 2006.

Eva Pluhařová, Henry E. Fischer, Philip E. Mason, and Pavel Jungwirth. Hydration of the chloride ion in concentrated aqueous solutions using neutron scattering and molecular dynamics. *Mol. Phys.*, 112(9-10):1230–1240, jan 2014. ISSN 0026-8976. doi: 10.1080/00268976.2013.875231. URL `http://www.tandfonline.com/doi/abs/10.1080/00268976.2013.875231`.

Kristýna Pluháčková, Sonja A. Kirsch, Jing Han, Liping Sun, Zhenyan Jiang, Tobias Unruh, and Rainer A. Böckmann. A Critical Comparison of Biomembrane Force Fields: Structure and Dynamics of Model DMPC, POPC, and POPE Bilayers. *Journal of Physical Chemistry B*, 120(16):3888–3903, apr 2016. ISSN 15205207. doi: 10.1021/acs.jpcb.6b01870. URL `http://pubs.acs.org/doi/10.1021/acs.jpcb.6b01870`.

Jay W Ponder, Chuanjie Wu, Pengyu Ren, Vijay S Pande, John D Chodera, Michael J Schnieders, Imran Haque, David L Mobley, Daniel S Lambrecht, Robert A DiStasio Jr, et al. Current status of the amoeba polarizable force field. *The journal of physical chemistry B*, 114(8):2549–2564, 2010.

R.P. Rand and V.A. Parsegian. Hydration forces between phospholipid bilayers. *Biochimica et Biophysica Acta (BBA) - Reviews on Biomembranes*, 988(3):351 – 376, 1989. ISSN 0304-4157. doi: https://doi.org/10.1016/0304-4157(89)90010-5. URL `http://www.sciencedirect.com/science/article/pii/0304415789900105`.

Michael Rappolt, Andrea Hickel, Frank Bringezu, and Karl Lohner. Mechanism of the lamellar/inverse hexagonal phase transition examined by high resolution x-ray diffraction. *Biophysical Journal*, 84(5):3111 – 3122, 2003. ISSN 0006-3495. doi: https://doi.org/10.1016/S0006-3495(03)70036-8. URL `http://www.sciencedirect.com/science/article/pii/S0006349503700368`.

Lorena Redondo-Morata, Gerard Oncins, and Fausto Sanz. Force spectroscopy reveals the effect of different ions in the nanomechanical behavior of phospholipid model membranes: The case of potassium cation. *Biophys. J.*, 102(1):66 – 74, 2012.

Sietze Reitsma, Dick W Slaaf, Hans Vink, Marc AMJ Van Zandvoort, and Mirjam GA Oude Egbrink. The endothelial glycocalyx: composition, functions, and visualization. *Pflügers Archiv-European Journal of Physiology*, 454(3):345–359, 2007.

Ken Ritchie, Yoriko Lill, Chetan Sood, Hochan Lee, and Shunyuan Zhang. Single-molecule imaging in live bacteria cells. *Phil. Trans. R. Soc. B*, 368(1611):20120355, 2013.

Benoît Roux. Influence of the Membrane potential on the free energy of an intrinsic protein. *Biophysical Journal*, 73(December):2980–2989, 1997.

Benoît Roux. The membrane potential and its representation by a constant electric field in computer simulations. *Biophys. J.*, 95(9):4205–16, November 2008. ISSN 1542-0086. doi: 10.1529/biophysj.108.136499.

Michel Roux and Myer Bloom. Calcium, magnesium, lithium, sodium, and potassium distributions in the headgroup region of binary membranes of phosphatidylcholine and phosphatidylserine as seen by deuterium nmr. *Biochemistry*, 29(30):7077–7089, 1990.

Jonathan N Sachs, Paul S Crozier, and Thomas B Woolf. Atomistic simulations of biologically realistic transmembrane potential gradients. *The Journal of chemical physics*, 121(22):10847–51, dec 2004a. ISSN 0021-9606. doi: 10.1063/1.1826056. URL `http://www.ncbi.nlm.nih.gov/pubmed/15634036http://scitation.aip.org/content/aip/journal/jcp/121/22/10.1063/1.1826056`.

Jonathan N. Sachs, Hirsh Nanda, Horia I. Petrache, and Thomas B. Woolf. Changes in phosphatidylcholine headgroup tilt and water order induced by monovalent salts: Molecular dynamics simulations. *Biophys. J.*, 86:3772 – 3782, 2004b.

Romelia Salomon-Ferrer, David A. Case, and Ross C. Walker. An overview of the amber biomolecular simulation package. *Wiley Interdisciplinary Reviews: Computational Molecular Science*, 3(2):198–210, 2013.

Peter G. Scherer and Joachim Seelig. Electric charge effects on phospholipid headgroups. phosphatidylcholine in mixtures with cationic and anionic amphiphiles. *Biochemistry*, 28:7720–7728, 1989.

PG Scherer and J Seelig. Structure and dynamics of the phosphatidylcholine and the phosphatidylethanolamine head group in l-m fibroblasts as studied by deuterium nuclear magnetic resonance. *EMBO J.*, 6(10):2915–2922, October 1987.

Russell Schwartz, Claire S Ting, and Jonathan King. Whole proteome pI values correlate with subcellular localizations of proteins for organisms within the three domains of life. *Genome research*, 11(5):703–709, 2001.

A. Seelig and J. Seelig. Effect of *cis* double bond on the structure of a phospholipid bilayer. *Biochemistry*, 16:45–50, 1977.

J Seelig. Interaction of phospholipids with ca^{2+} ions. on the role of the phospholipid head groups. *Cell Biol. Int. Rep.*, 14(4):353–360, April 1990. URL `http://dx.doi.org/10.1016/0309-1651(90)91204-H`.

Joachim Seelig and Hans U. Gally. Investigation of phosphatidylethanolamine bilayers by deuterium and phosphorus-31 nuclear magnetic resonance. *Biochemistry*, 15(24):5199–5204, 1976. doi: 10.1021/bi00669a001. URL `https://doi.org/10.1021/bi00669a001`. PMID: 11810.

Joachim Seelig, Peter M. MacDonald, and Peter G. Scherer. Phospholipid head groups as sensors of electric charge in membranes. *Biochemistry*, 26(24):7535–7541, 1987.

Juraj Sekereš, Roman Pleskot, Přemysl Pejchar, Viktor Žárský, and Martin Potocký. The song of lipids and proteins: dynamic lipid–protein interfaces in the regulation of plant cell polarity at different scales. *Journal of experimental botany*, 66(6):1587–1598, 2015.

Yue Shi, Zhen Xia, Jiajing Zhang, Robert Best, Chuanjie Wu, Jay W Ponder, and Pengyu Ren. Polarizable atomic multipole-based AMOEBA force field for proteins. *Journal of chemical theory and computation*, 9(9):4046–4063, 2013.

Jun-Sik Sin, Song-Jin Im, and Kwang-Il Kim. Asymmetric electrostatic properties of an electric double layer: a generalized Poisson-Boltzmann approach taking into account non-uniform size effects and water polarization. *Electrochim. Acta*, 153:531–539, January 2015. ISSN 00134686. doi: 10.1016/j.electacta.2014.11.119. URL `http://www.sciencedirect.com/science/article/pii/S001346861402338X`.

U. Chandra Singh and Peter A. Kollman. An approach to computing electrostatic charges for molecules. *J. Comput. Chem.*, 5(2):129–145, 1984. ISSN 1096987X. doi: 10.1002/jcc.540050204.

Ove Sten-Knudsen. *Biological Membranes: Theory of Transport, Potentials and Electric Impulses.* Cambridge University Press, 2002. ISBN 0521810183. URL `http://researchbooks.org/0521810183`.

Douglas Storace, Masoud Sepehri Rad, Zhou Han, Lei Jin, Lawrence B Cohen, Thom Hughes, Bradley J Baker, and Uhna Sung. Genetically Encoded Protein Sensors of Membrane Potential. *Advances in experimental medicine and biology*, 859:493–509, jan 2015. ISSN 0065-2598. doi: 10.1007/978-3-319-17641-3_20. URL `https://www.researchgate.net/publication/280694860_Genetically_Encoded_Protein_Sensors_of_Membrane_Potential`.

Uhna Sung, Masoud Sepehri-Rad, Hong Hua Piao, Lei Jin, Thomas Hughes, Lawrence B Cohen, and Bradley J Baker. Developing Fast Fluorescent Protein Voltage Sensors by Optimizing FRET Interactions. *PloS one*, 10(11): e0141585, jan 2015. ISSN 1932-6203. doi: 10.1371/journal.pone.0141585. URL `https://www.researchgate.net/publication/284278145_Developing_Fast_Fluorescent_Protein_Voltage_Sensors_by_Optimizing_FRET_Interactions`.

Orly B Tarun, Christof Hannesschläger, Peter Pohl, and Sylvie Roke. Label-free and charge-sensitive dynamic imaging of lipid membrane hydration on millisecond time scales. *Proceedings of the National Academy of Sciences*, 115 (16):4081–4086, 2018.

D.P. Tieleman, H.J.C. Berendsen, and M.S.P. Sansom. Voltage-Dependent Insertion of Alamethicin at Phospholipid/Water and Octane/Water Interfaces. *Biophys. J.*, 80(1):331–346, January 2001. ISSN 00063495. doi: 10.1016/S0006-3495(01)76018-3. URL `http://www.researchgate.net/publication/12171102_Voltage-Dependent_Insertion_of_Alamethicin_at_PhospholipidWater_and_OctaneWater_Interfaces`.

Štěpán Timr, Jan Kadlec, Pavel Srb, O. H. Samuli Ollila, and Pavel Jungwirth. Calcium Sensing by Recoverin: Effect of Protein Conformation on Ion Affinity. *The journal of physical chemistry letters*, 9(7):1613–1619, 2018.

Jean-François Tocanne and Justin Teissié. Ionization of phospholipids and phospholipid-supported interfacial lateral diffusion of protons in membrane model systems. *Biochim. Biophys. Acta*, 1031(1):111 – 142, 1990.

Daniela Uhríková, Norbert Kučerka, J. Teixeira, Valentin Gordeliy, and Pavol Balgavý. Structural changes in dipalmitoylphosphatidylcholine bilayer promoted by ca^{2+} ions: a small-angle neutron scattering study. *Chem. Phys. Lipids*, 155(2):80 – 89, 2008.

Brooke L Urquhart, Stuart J Cordwell, and Ian Humphery-Smith. Comparison of Predicted and Observed Properties of Proteins Encoded in the Genome of Mycobacterium Tuberculosis H37Rv. *Biochemical and biophysical research communications*, 253(1):70–79, 1998.

Robert Vacha, Shirley W. I. Siu, Michal Petrov, Rainer A. Böckmann, Justyna Barucha-Kraszewska, Piotr Jurkiewicz, Martin Hof, Max L. Berkowitz, and Pavel Jungwirth. Effects of Alkali Cations and Halide Anions on the DOPC Lipid Membrane. *J. Phys. Chem. A*, 113:7235–7243, 2009.

Christopher C. Valley, Jason D. Perlmutter, Anthony R. Braun, and Jonathan N. Sachs. Nacl interactions with phosphatidylcholine bilayers do not alter membrane structure but induce long-range ordering of ions and water. *J. Membr. Biol.*, 244:35–42, 2011.

Floris J Van Eerden, Manuel N Melo, Pim WJM Frederix, Xavier Periole, and Siewert J Marrink. Exchange pathways of plastoquinone and plastoquinol in the photosystem ii complex. *Nature communications*, 8:15214, 2017.

Gerrit van Meer and Anton IPM de Kroon. Lipid map of the mammalian cell. *J Cell Sci*, 124(1):5–8, 2011.

Ernesto Vargas, Vladimir Yarov-Yarovoy, Fatemeh Khalili-Araghi, William A Catterall, Michael L Klein, Mounir Tarek, Erik Lindahl, Klaus Schulten, Eduardo Perozo, Francisco Bezanilla, and Benoît Roux. An emerging consensus on voltage-dependent gating from computational modeling and molecular dynamics simulations. *J. Gen. Physiol.*, 140(6):587–94, dec 2012. ISSN 1540-7748. doi: 10.1085/jgp.201210873. URL `http://jgp.rupress.org/content/140/6/587.long`.

Ilpo Vattulainen and Tomasz Rog. Lipid simulations: a perspective on lipids in action. *Cold Spring Harb. Perspect. Biol.*, 3(4):a004655, April 2011. ISSN 1943-0264. doi: 10.1101/cshperspect.a004655. URL `http://cshperspectives.cshlp.org/content/3/4/a004655.full`.

Richard M. Venable, Yun Luo, Klaus Gawrisch, Benoît Roux, and Richard W. Pastor. Simulations of Anionic Lipid Membranes: Development of Interaction-Specific Ion Parameters and Validation Using NMR Data. *J. Phys. Chem. B*, 117(35):10183–10192, 2013.

G Vereb, J Szöllosi, J Matkó, P Nagy, T Farkas, L Vigh, L Mátyus, T A Waldmann, and S Damjanovich. Dynamic, yet structured: The cell membrane three decades after the Singer-Nicolson model. *Proceedings of the National Academy of Sciences of the United States of America*, 100(14):8053–8, jul 2003. ISSN 0027-8424. doi: 10.1073/pnas.1332550100. URL `http://www.pnas.org/content/100/14/8053`.

Hui-Jun Wang, Ginette Guay, Liviu Pogan, Remy Sauvé, and Ivan R. Nabi. Calcium Regulates the Association between Mitochondria and a Smooth Subdomain of the Endoplasmic Reticulum. *The Journal of Cell Biology*, 150(6): 1489–1498, sep 2000. ISSN 0021-9525. doi: 10.1083/jcb.150.6.1489. URL `http://www.jcb.org/lookup/doi/10.1083/jcb.150.6.1489`.

Roland Wohlgemuth, Nada Waespe-Sarcevic, and Joachim Seelig. Bilayers of phosphatidylglycerol. a deuterium and phosphorus nuclear magnetic resonance study of the head-group region. *Biochemistry*, 19(14):3315–3321, 1980. doi: 10.1021/bi00555a033. URL `https://doi.org/10.1021/bi00555a033`. PMID: 7407046.

Wenlei Ye, Tina W Han, Layla M Nassar, Mario Zubia, Yuh Nung Jan, and Lily Yeh Jan. Phosphatidylinositol-(4, 5)-bisphosphate regulates calcium gating of small-conductance cation channel tmem16f. *Proceedings of the National Academy of Sciences*, 115(7):E1667–E1674, 2018.

Johan. Åqvist. Ion-water interaction potentials derived from free energy perturbation simulations. *J. Phys. Chem.*, 94(21):8021–8024, 1990. doi: 10.1021/j100384a009. URL `http://dx.doi.org/10.1021/j100384a009`.

List of Figures

2.1 Top: X-ray scattering form factors from simulations with the Lipid14 [Dickson et al., 2014] and the ECC-POPC [Melcr et al., 2018] models compared with experiments [Kučerka et al., 2011] at 303 K. Middle: Order parameters of POPC head group, glycerol backbone and acyl chains from simulations with the Lipid14 and the ECC-POPC models compared with experiments [Ferreira et al., 2013] at 300 K. The size of the markers for the head group order parameters correspond to the error estimate ±0.02 for experiments [Botan et al., 2015, Ollila and Pabst, 2016], while the error estimate for simulations is ±0.005 (Bayesian estimate of 95% confidence interval [Jones et al., 2001–2018]). The size of the points for acyl chains are decreased by a factor of 3 to improve the clarity of the plot. Open/closed symbols are used for palmitoyl/oleoyl chains of POPC. Bottom: The chemical structure of POPC and the labeling of the carbon segments. 15

2.2 Top: X-ray scattering form factors from simulations with the ECC-lipids model of POPE compared with experiments Kučerka et al. [2011] at 313 K. Bottom: Order parameters of POPE head group, glycerol backbone and acyl chains from simulations with the ECC-lipids model of POPE compared with experiments by Gally et al. [1981] (order parameters of glycerol backbone, labeled *E. coli* membrane at 310 K,) and by Seelig and Gally [1976], Wohlgemuth et al. [1980] (order parameters α and β from DPPE at 341 K). The signs of the order parameters were not determined in the experiments, same signs as in POPC (Fig. 2.1) are assumed. Open/closed symbols are used for palmitoyl/oleoyl chains of POPE. The chemical structure of POPE is the same as for POPC in Fig. 2.1, but the methyl groups in choline (denoted with γ), which are substituted with hydrogen atoms in PE. 16

2.3 Top: X-ray scattering form factors from simulations with the Lipid17 [Gould et al., 2018] and the ECC-POPS models compared with experiments [Pan et al., 2014] at 298 K. Middle: Order parameters of POPS head group, glycerol backbone and acyl chains from simulations with the Lipid17 [Gould et al., 2018] and the ECC-POPS models compared with experiments at 298 K. [Bacle et al., 2018] Open/closed symbols are used for palmitoyl/oleoyl chains of POPS. Bottom: The chemical structure of POPS and the labeling of the carbon segments. 17

2.4 The transmembrane potential (A,B), the electric field intensity (C,D), and the charge density (E,F) profiles for simulations of a POPC bilayer with 150 mM concentration of KCl. ZERO stands for simulations without any applied voltage, IIMB stands for the ion imbalance method, CEF stands for the constant electric field method, and FxI denotes the special setup, in which the two methods are applied simultaneously. The gray area shows the standard error. The voltage drop across the membrane is 499 mV for IIMB and 486 mV for CEF with the error of about 7 mV. 19

3.1 Changes of the head group order parameters β (top row) and α (bottom row) to increasing concentrations of NaCl (left column) and $CaCl_2$ (right column) Results from experiments (DPPC from Ref. [Akutsu and Seelig, 1981], POPC from Ref. [Altenbach and Seelig, 1984]) are compared with simulations with different force fields [Miettinen and Ollila, 2018, Catte et al., 2016]. Note that none of the employed models in this figure reproduces the order parameters without any salt concentration within experimental error, indicating structural inaccuracies of varying severity in all of them [Botan et al., 2015]. 23

3.2 Changes of the head group order parameters α, β and P-N vector orientation as a function of the molar fraction of a cationic surfactant dihexadecyldimethylammonium in a POPC bilayer from simulations and experiments [Scherer and Seelig, 1989] at 313 K. 24

3.3 Changes of head group order parameters α and β and P-N vector orientation in a POPC bilayer as a function of NaCl (left) and KCl (right) concentration in bulk (C_{ion}) from simulations with different force fields at 313 K together with experimental data for DPPC (323 K) [Akutsu and Seelig, 1981] and POPC (313 K) [Altenbach and Seelig, 1984]. Simulation data with Lipid14 and Åqvist ion parameters at 298 K are taken directly from Refs. [Girych and Ollila, 2015a,b]. 25

3.4 Changes of the head group order parameters α, β and the orientations of the carboxylate group and the P-N vector of POPC (left) and POPS (right) phospholipids in a POPC:POPS 5:1 bilayer as a function of NaCl concentration in bulk (C_{ion}) from simulations with different force fields at 298 K. Because data with NaCl are not available for POPC, we show experimental data for LiCl (dashed line, left) as an upper bound for the magnitude of the response to NaCl, which has a lower affinity to phospholipid bilayers compared to LiCl [Roux and Bloom, 1990]. The orientation of the COO^- group is defined as the connector from the β carbon to the carbon in COO^- (stars, bottom right). 26

3.5 Changes of the head group order parameters α, β and the orientations of the carboxylate group and the P-N vector of POPC (left) and POPS (right) phospholipids in a POPC:POPS 5:1 bilayer as a function of KCl concentration in bulk (C_{ion}) from simulations with different force fields and experiments at 298 K. [Roux and Bloom, 1990] The orientation of the COO^- group is defined as the connector from the β carbon to the carbon in COO^- (stars, bottom right). 27

3.6 Number density profiles of K^+, Na^+ and Cl^- along the membrane normal axis from the simulations with the neutral POPC bilayer using ECC-lipids and ECC-ions. In order to visualize the density profiles with a scale comparable to the profile of Ca^{2+} in Fig. 3.10, the density profiles of Cl^-, K^+ and Na^+ ions are divided by 2, and the density profiles of phosphate groups and water are divided by 5 and 200, respectively. Both simulations have the same molar fractions of NaCl resp. KCl in water, C'_{ion}=1000 mM. 29

3.7 Number density profiles of K^+, Na^+ and Cl^- along the membrane normal axis for the negatively charged membranes with the composition of 5 PC:1 PS using ECC-lipids and ECC-ions. The top profile shows the simulation without any additional salt concentration, i.e., only with Na^+ counterions. The middle profile shows the simulation with an additional KCl concentration and Na^+ counterions. The bottom profile shows the simulation with an additional NaCl concentration and Na^+ counterions, which are not distinguished from the added salt. In order to visualize the density profiles with a scale comparable to the profile of Ca^{2+} in Fig. 3.10, the density profiles of Cl^-, K^+ and Na^+ ions are divided by 2, and the density profiles of phosphate groups and water are divided by 5 and 200, respectively. 30

3.8 Changes of the head group order parameters and P-N vector orientation of a POPC bilayer as a function of the $CaCl_2$ concentration in bulk (C_{ion}) from simulations at 313 K together with experimental data (DPPC (323 K) [Akutsu and Seelig, 1981] and POPC (313 K) [Altenbach and Seelig, 1984]). The error estimate for bulk concentrations is approximately 10 mM. The order of magnitude larger error in the simulation with Lipid14 and ECC-ions is due to unconverged bulk densities limited by the simulation box. Simulation data with Lipid14 and Åqvist ion parameters at 298 K are taken directly from Refs. [Girych and Ollila, 2015a,c, 2016]. . . . 31

3.9 Changes of the head group order parameters α, β and the orientations of the carboxylate group and the P-N vector of POPC (left) and POPS (right) phospholipids in a POPC:POPS 5:1 bilayer as a function of $CaCl_2$ concentration in bulk (C_{ion}) from simulations with different force fields and experiments at 298 K. [Roux and Bloom, 1990] The orientation of the COO^- group is defined as the connector from the β carbon to the carbon in COO^- (stars, bottom right). 32

3.10 Number density profiles of Ca^{2+} and Cl^- along the normal of the neutral POPC bilayers starting at the centre for different concentrations of $CaCl_2$ from simulations with ECC-lipids. In order to visualize the density profiles with a scale comparable to the profile of Ca^{2+}, the density profiles of Cl^- ions are divided by 2, and the density profiles of phosphate groups and water are divided by 5 and 200, respectively. 34

3.11 Number density profiles of Ca^{2+}, Na^+ and Cl^- along the normal of the membrane starting at the centre for the negatively charged membrane with the composition 5 PC:1 PS at various bulk concentrations of $CaCl_2$ from simulations with ECC-lipids. All profiles contain Na^+ counterions and an additional concentration of $CaCl_2$. In order to visualize the density profiles with a scale comparable to the profile of Ca^{2+}, the density profiles of Cl^- ions are divided by 2, and the density profiles of phosphate groups and water are divided by 5 and 200, respectively. 35

3.12 Isocontours of spatial number density of Ca^{2+} (dark blue, 0.001 $Å^{-3}$) and POPC carbonyl oxygen atoms (light semi-transparent red, 0.008 $Å^{-3}$, all POPC lipids contribute). Calcium cations localize mostly around phosphate oxygens (oxygens red, phosphorus bronze). Interactions with carbonyl oxygens is less likely than with phosphate oxygens, and it is contributed more by other neighbouring phospholipids than by the same lipid. Transparent structures are shown to depict the variability of choline configurations (colour warps from red to blue along the simulation time). The number density was evaluated for each lipid, after its structural alignment using only phosphate group. MDAnalysis [Michaud-Agrawal et al., 2011] library was used for the calculations of the structural alignment and the spatial number density. VMD [Humphrey et al., 1996] was used for visualization. Carbon atoms are depicted in cyan, hydrogen atoms in white, oxygen atoms in red, nitrogen in blue. 37

3.13 Relative probabilities of existence of Ca^{2+} complexes with a certain number of lipids. All lipids were taken into account with the exception of the complexes in light green and orange, for which we counted only contacts with POPC resp POPS from the mixed 5 PC:1 PS negatively charged bilayer. The calculated probabilities of the calcium-lipid complexes also reflect only POPC (light green) resp POPS (orange). Probabilities were taken from simulations with comparable bulk concentrations of calcium around 250 mM. Clusters of four or more lipids were not observed in either membrane. 38

3.14 Histograms of residence times of Ca^{2+} in a neutral membrane composed of POPC (orange) and in a negatively charged membrane with the composition 5 PC:1 PS (blue) from simulations with ECC-lipids and ECC-ions. The simulation with the neutral membrane has a bulk concentration of calcium $C_{ion} = 280$mM, the simulation with the negatively charged membrane has a bulk concentration of calcium $C_{ion} = 240$mM. In the simulation with the neutral membrane, 90% of the residence times of calcium cations are shorter than 60 ns, with the longest observed residence time being 141 ns. In the simulation with the negatively charged membrane, 90% of the residence times of calcium cations are shorter than 200 ns, with the longest observed residence time being 485 ns. 38

List of Tables

2.1 Values of the area per lipid (APL) of POPC, POPE and POPS bilayers at temperatures T without additional ions. 18

3.1 Bulk concentrations, C_{Ca}, and molar fractions, C'_{Ca}, of Ca^{2+}; relative surface excess of calcium with respect to water ($\Gamma_{Ca}^{\mathrm{water}}$); and percentages of the population of bound Ca^{2+} to various moieties in a neutral membrane composed of POPC and in a negatively charged membrane with the composition 5 PC:1 PS. 36

List of Abbreviations

MD Molecular dynamics

ECC Electronic continuum correction

POPC Palmitoyloleoylphosphatidylcholine

DPPC Dipalmitoylphosphatidylcholine

POPS Palmitoyloleoylphosphatidylserine

POPE Palmitoyloleoylphosphatidylethanolamine

PC Phosphatidylcholine

PS Phosphatidylserine

PE Phosphatidylethanolamine

NMR Nuclear Magnetic Resonance

List of publications and attachments

I Transmembrane Potential Modeling: Comparison between Methods of Constant Electric Field and Ion Imbalance. Journal of Chemical Theory and Computation, 12(5), (2016). Josef Melcr, Daniel Bonhenry, Štěpán Timr, and Pavel Jungwirth.

II Molecular electrometer and binding of cations to phospholipid bilayers. Phys. Chem. Chem. Phys., (2016). Andrea Catte, Mykhailo Girych, Matti Javanainen, Claire Loison, Josef Melcr, Markus S. Miettinen, Luca Monticelli, Jukka Maatta, Vasily S. Oganesyan, O. H. Samuli Ollila, Joona Tynkkynen, and Sergey Vilov.

III Accurate Binding of Sodium and Calcium to a POPC Bilayer by Effective Inclusion of Electronic Polarization. (2018) The Journal of Physical Chemistry B, 122(16), (2018). Josef Melcr, Hector Martinez-Seara, Ricky Nencini, Jiří Kolafa, Pavel Jungwirth, and O. H. Samuli Ollila.

IV Head group and glycerol backbone structures, and cation binding in bilayers with PS lipids. Submitted (2018). Amelie Bacle, Pavel Buslaev, Lukasz Cwiklik, Fernando Favela, Tiago Ferreira, Patrick Fuchs, Ivan Gushchin, Matti Javanainen, Batuhan Kav, Jesper Madsen, Josef Melcr, Markus Miettinen, Ricky Nencini, Chris Papadopoulos, Thomas Piggot and O. H. Samuli Ollila.